Abstract

Subject of this work is the investigation of inverse problems related to the transient drift - diffusion equations modeling semiconductor devices.
We discuss the identification of the doping profile from indirect transient measurements. In case of current and capacitance measurement we prove that all involved operators are well-defined, continuous and Fréchet differentiable. For Tikhonov based regularization methods we show that a regularized solution exists.
In addition, a reduced model obtained by asymptotic expansion of the drift - diffusion equations is considered, which leads to the special case of identifying piecewise constant doping profiles.
We present uniqueness and non-uniqueness results for regularized solutions. Furthermore the construction of descent algorithms employing the adjoint state and their numerical performance is discussed.

Zusammenfassung

Die vorliegende Arbeit beschäftigt sich mit inversen Problemen im Zusammenhang mit der mathematischen Modellierung von Halbleitern, die durch die Drift-Diffusionsgleichungen beschrieben werden können.
Wir befassen uns mit der Fragestellung, wie sich das Dotierungsprofil eines Halbleiters aus zeitabhängigen Messungen rekonstruieren lässt. Für Strom- und Kapazitätsmessungen zeigen wir, dass alle verwendeten Operatoren wohl-definiert, stetig und Fréchet differenzierbar sind. Weiters wird die Existenz einer Lösung für Tikhonov basierte Regularisierungsverfahren gezeigt.
Im Falle stark dotierter Halbleiter führen wir eine asymptotische Entwicklung der Drift-Diffusionsgleichungen durch und behandeln den Spezialfall stückweiser stetiger Dotierungsprofile.
Wir betrachten Eindeutigkeits- und Nichteindeutigkeitsresultate für unipolare und bipolare Dioden. Weiters diskutieren wir die adjungierte Methode zur Gradientenberechnung, gradientenbasierte Optimierungsverfahren und präsentieren numerische Ergebnisse.

Acknowledgments

First of all I would like to thank my adviser Dipl.-Ing. Dr. Martin Burger, who initiated my work in inverse problems related to semiconductor devices. His guidance and constructive comments have been a great help for me.
Furthermore I want to express my gratitude to Prof. Heinz Engl and the Institute for Pure and Applied Mathematics at the UCLA, for giving me the opportunity to present my work at the IPAM reunion conference in Lake Arrowhead. I want to thank the staff of the Industrial Mathematics Institute for their motivation and helpful responses to all my questions.
During the last year I had lively discussions with Markus Bachmayr about all kinds of mathematical questions. These discussions have been supporting for my work until now.
I want to thank my family, especially my parents, for their steady confidence and their support through all the years. Last but not least I would like to thank Günther for his understanding and encouragement.

Contents

Chapter 1

Introduction

In recent years there has been a growing demand in industry for mathematical modeling of semiconductor devices. The first fundamental semiconductor device equations were introduced by Van Roosbroeck in 1950 and are mathematically quite well understood. For detailed derivation of the underlying models and analysis we refer to the works [17] and [16]. There has been a lot of work done in numerical simulations of the drift -diffusion equations, in order to reduce development time in semiconductor design.
Identification and optimal design problems related to semiconductor devices have been investigated concerning steady state models. There has been recent work on the optimizing the performance of devices (cf. e.g. [15],[5]) and in identifying relevant material properties (cf. e.g. [4],[3],[2]).
The quantity to be optimized or identified is the doping profile C, which is the density difference of ionized donors and acceptors. $C = C(x)$ may be assumed to be a piecewise constant function - then the quantity of interest is the region between the sub domains where C is constant, the so called pn-junction.

The inverse dopant problem refers to the reconstruction of the doping profile from indirect measurements. Several types of measurements are introduced in literature like the capacitance measurements, the voltage current map or laser beam induced currents. In this work the reconstruction of the doping profile from time-dependent measurements of the current and the capacitance is discussed. Further-

more the case of heavily doped semiconductor devices is investigated, which can be seen as a singular perturbation limit for several parameters tending to zero. In this case the doping profile is assumed to be a piecewise constant function and the quantity to be identified is the pn-junction.

This work is organized as follows. In Chapter 2 the basic properties of semiconductor devices are introduced shortly. Chapter 3 describes the transient drift - diffusion equations, their underlying analysis and the singular perturbation analysis carried out for heavily doped semiconductors.
The inverse problem of reconstructing the doping profile from indirect measurements is presented in Chapter 4. Furthermore the adjoint approach, used for gradient evaluation is introduced shortly and regularization methods are discussed. The identifiability of the doping profile from indirect measurements is discussed in Chapter 5. Furthermore non-uniqueness results for regularized solutions are presented concerning simplified cases.
In Chapter 6 the special case of identifying piecewise constant doping profiles of unipolar or bipolar diodes is investigated. The main aim is the reconstruction of the pn-junction that marks the discontinuity of the doping profile. This problem corresponds to so called inverse boundary problems in literature.
In Chapter 7 we present numerical examples and discuss the results.

Chapter 2

Basic Properties of Semiconductor Devices

The Bohr model of an atom consists of a positively charged nucleus and a system of negatively charged electrons which rotate around it. The electrons are bounded to the nucleus by forces of attraction of oppositely charged particles. They are arranged in shells with every shell containing a maximum number of electrons. The outer shell can have no more than eight electrons which are called valence electrons. If a valence electron escapes from its parent atom it becomes free to move. Depending on the number of free valence electrons per unit volume a solid is classified as conductor, semiconductor or insulator. Semiconductors are the

Table 2.1: Typical number of free valence electrons at $T = 300K$

		number of free valence electrons
Insulator	diamond	10^6
Semiconductor	silicon, germanium	10^{16}
Conductor	metals	10^{26}

class of elements that contain four valence electrons. Applying an electric field or raising the temperature causes the covalent bonds to break - valence electrons become conduction electrons, leaving a 'hole'. The holes are considered as pos-

Figure 2.1: Implantation of impurity atoms into the semiconductor crystal

(a) Donors (b) Acceptors

itively charged carriers, the conduction electrons as negatively charged carriers. The movement of the holes as well as the movement of the conduction electrons causes an electrical current called conduction or drift current. Because of the smaller number of free valence electrons the conductivity of a semiconductor is smaller than of a conductor. To increase the conductivity impurity atoms are implanted into the semiconductor crystal - this process is called 'doping'. Atoms, which can either produce one or more excess conduction electrons (called donors) or accept electrons and produce holes (called acceptors), can be implemented into semiconductor crystals, see Figure 2. The distribution of donors and acceptors de-

Figure 2.2: np-Diode forward and reverse bias

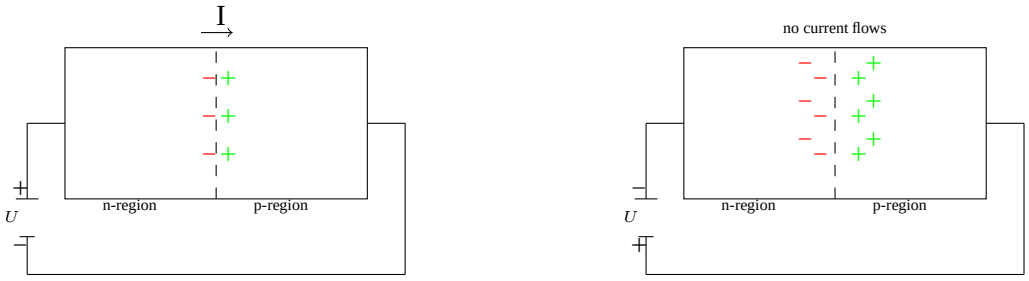

(a) forward bias (b) reverse bias

termines the performance of the semiconductor. Parts of the semiconductor that are dominantly doped with acceptors are called p-regions, regions that are dominantly doped with donors n-regions. The difference of the concentration of donor and acceptor atoms is called the doping profile $C = C(x)$ of a semiconductor

device. In p-regions $C < 0$ holds, in n-regions $C > 0$.

Most basic semiconductors consist of combinations of n and p-regions. The simplest model is a np-diode - a combination of a n-region and a p-region. At the junction of both regions, the so called pn-junction, the holes and electrons combine and a small layer with no charge arises. Depending on the sign of the applied bias the semiconductor acts like a 'valve'. Applying a positive bias to the n-region causes a large current to flow. The application of a negative bias causes the electrons and holes to draw back - the pn-layer becomes larger and no current can flow. Both cases can be seen in Figure 2.2.

Chapter 3

The Drift-Diffusion Equations

The most commonly used model to describe semiconductor devices are the drift-diffusion equations, first introduced by Roosbroeck in 1950. Today industry is interested in replacing much of laboratory work by numerical simulations for the purpose of minimizing costs. In order to compute numerical solutions in a reasonable amount of time, the mathematical models cannot be too complicated. The drift-diffusion equations seem to be a reasonable compromise between computational efficiency and accurate description of the underlying device physics for an important range of device sizes and parameters.
With the ongoing minimization of semiconductor devices the drift diffusion equations are getting to the limits of validity. Quantum effects become more important and some assumptions the drift diffusion equations are based on do not hold any more. Different mathematical models for semiconductor devices are the quantum-hydrodynamical model or the Boltzmann equations .
The drift diffusion model stated on a bounded domain $\Omega \subset \mathbb{R}^d, d = 1, 2, 3$ reads

$$\operatorname{div}(\epsilon \operatorname{grad} V) = q(n - p - C) \tag{3.1a}$$

$$\operatorname{div} J_n = q\left(\partial_t n + R\right) \tag{3.1b}$$

$$\operatorname{div} J_p = q\left(-\partial_t p - R\right) \tag{3.1c}$$

$$J_n = q\left(D_n \operatorname{grad} n - \mu_n n \operatorname{grad} V\right) \tag{3.1d}$$

$$J_p = q\left(-D_p \operatorname{grad} p - \mu_p p \operatorname{grad} V\right) \tag{3.1e}$$

The variables are the electrical potential V ($E = -\operatorname{grad} V$ denotes the electric field), the concentrations of free negatively charged carriers n (called electrons) and positively charged carriers p (called holes). C is the predefined doping profile of the semiconductor and therefore a function of the spatial variable only. J_n and J_p are the current densities of electrons and holes. The total current density J is given by

$$J = J_n + J_p \tag{3.2}$$

The parameters $D_n,\ D_p, \mu_n$ and μ_p are the diffusion coefficients and mobilities of electrons and holes respectively. In general they depend on the strength of the electric field and can be modeled as positive functions - for the sake of simplicity they are assumed to by constants in the following. ϵ and q are the permittivity constant and the elementary charge, both positive functions.

R is the recombination-generation rate. Recombination takes place when a conduction electrons becomes a valence electron, generation when a valence electron becomes a conduction electron. The recombination-generation rate can be interpreted as the difference of the rate at which electron-hole carrier pairs recombine and the rate at which they are generated in the semiconductor. Several models can be found in literature, we shall consider the Shockley-Read-Hall (SRH) recombination-generation rate

$$R_{SRH} = \frac{np - n_i^2}{\tau_p(n + n_i) + \tau_n(p + n_i)} \tag{3.3}$$

or the Auger recombination rate

$$R_{AU} = (C_n n + C_p p)\,(np - n_i^2) \tag{3.4}$$

where n_i denotes the intrinsic density, τ_n and τ_p are the lifetimes of the electrons and holes respectively .

The boundary is divided in two parts - the Dirichlet part $\partial\Omega_D$ and the Neumann part $\partial\Omega_N$:

$$\partial\Omega = \partial\Omega_N \ \cup\ \partial\Omega_D, \quad \partial\Omega_D \ \cap\ \partial\Omega_N = \emptyset$$

At the Ohmic contacts (which correspond to the Dirichlet part) the following assumptions are made:

1. The space charge given by right hand side of (3.1a) vanishes
2. The system is in thermal equilibrium.

These assumptions are expressed by the following equations:

$$n - p - C = 0 \quad x \in \partial\Omega_D$$
$$np = n_i^2 \quad x \in \partial\Omega_D$$

This implies the following type of boundary conditions on $\partial\Omega_D$:

$$n(x,t) = n_D(x) = \frac{1}{2}(C(x) + \sqrt{C(x)^2 + 4n_i^2}) \tag{3.5a}$$
$$p(x,t) = p_D(x) = \frac{1}{2}(-C(x) + \sqrt{C(x)^2 + 4n_i^2}) \tag{3.5b}$$
$$V(x,t) = V_D(x,t) = U(x,t) + U_T \ln \frac{n_D(x)}{n_i} \tag{3.5c}$$

Here U_T is the thermal voltage and $U(x,t)$ denotes the applied potential.
The Neumann parts $\partial\Omega_N$ model insulating surfaces. Therefore no current flows in normal direction and the normal component of the electric field vanishes. The following boundary conditions hold on $\partial\Omega_N$:

$$\frac{\partial V}{\partial \nu} = 0 \tag{3.6a}$$
$$J_n(x,t) \cdot \nu = 0 \tag{3.6b}$$
$$J_p(x,t) \cdot \nu = 0 \tag{3.6c}$$

Here ν denotes the unit outward normal vector on the boundary $\partial\Omega$.
Initial condition for the free carrier concentrations n and p at $t = 0$ are:

$$n(x,0) = n^I(x) \qquad p(x,0) = p^I(x) \qquad x \in \Omega. \tag{3.7}$$

3.1 Scaling

In order to obtain the dimensionless formulation of the drift-diffusion equations the following scaling, as recommended by [17], is proposed.
Suppose the geometry has a characteristic length scale L. The scaling

$$x = Lx_s \tag{3.8}$$

is used for the position variable x. The dependent variables $n,\ p,\ V,\ J_n$ and J_p are scaled as follows:

$$V = U_T\, V_s \qquad n = \tilde{C}\, n_s \qquad p = \tilde{C}\, p_s \tag{3.9}$$

$$J_n = \frac{q\, U_T\, \tilde{C}\, \tilde{\mu}}{L}\, J_{n_s} \qquad J_p = \frac{q\, U_T\, \tilde{C}\, \tilde{\mu}}{L}\, J_{p_s} \tag{3.10}$$

The subscript s denotes the scaled and dimensionless variables. $\tilde{C}$ denotes the maximal absolute value of the doping concentration which in typical applications ranges from $10^{15}\ \mathrm{cm}^{-3}$ to $10^{21}\ \mathrm{cm}^{-3}$. $\tilde{\mu}$ is a characteristic value for the mobilities μ_n and μ_p, usually of the order of $1000\ \mathrm{cm}^2\mathrm{V}^{-1}\mathrm{s}^{-1}$. Furthermore the Einstein relations

$$D_n = U_T \mu_n, \qquad D_p = U_T \mu_p \tag{3.11}$$

are assumed to hold and we set

$$\mu_n = \tilde{\mu}\mu_{ns}, \qquad \mu_p = \tilde{\mu}\mu_{ps} \tag{3.12}$$

Using this scaling and assuming that ϵ is constant, we obtain the scaled drift-diffusion equations

$$\lambda^2 \triangle V_s = n_s - p_s - C_s \tag{3.13a}$$

$$\frac{L^2}{U_T \tilde{\mu}} \partial_t n_s = \operatorname{div} J_{n_s} - R_s \tag{3.13b}$$

$$\frac{L^2}{U_T \tilde{\mu}} \partial_t p_s = -\operatorname{div} J_{p_s} - R_s \tag{3.13c}$$

$$J_{n_s} = \mu_{n_s}(\operatorname{grad} n_s - n_s\ \operatorname{grad} V_s) \tag{3.13d}$$

$$J_{p_s} = \mu_{p_s}(-\operatorname{grad} p_s - p_s\ \operatorname{grad} V_s) \tag{3.13e}$$

R_s is the scaled Shockley-Read-Hall term of the form:

$$R_s = \frac{n_s p_s - \sigma^4}{\tau_{p_s}(n_s + \sigma^2) + \tau_{n_s}(p_s + \sigma^2)} \tag{3.14}$$

The scaled Dirichlet boundary conditions on $\partial\Omega_{D_s}$ are

$$\begin{aligned} n_s(x,t) &= n_{D_s}(x) = \frac{1}{2}(C_s(x) + \sqrt{C_s(x)^2 + 4\sigma^4}) \\ p_s(x,t) &= p_{D_s}(x) = \frac{1}{2}(-C_s(x) + \sqrt{C_s(x)^2 + 4\sigma^4}) \\ V_s(x,t) &= V_{D_s}(x,t) = U_s(x,t) + V_{bi_s}(x) \\ V_{bi_s}(x) &= \ln(\frac{1}{2\sigma^2}(C_s(x) + \sqrt{C_s(x)^2 + 4\sigma^4})) \end{aligned} \tag{3.15a}$$

and the scaled Neumann boundary conditions on $\partial\Omega_{N_s}$

$$\begin{aligned} &\frac{\partial V_s}{\partial \nu} = 0 \\ &J_{n_s}(x,t) \cdot \nu = 0 \\ &J_{p_s}(x,t) \cdot \nu = 0 \end{aligned} \tag{3.15b}$$

The parameters λ, the so-called Debye length of the device, and σ are given by:

$$\lambda = \left(\frac{\epsilon U_T}{q\tilde{C}L^2}\right)^{\frac{1}{2}} \qquad\qquad \sigma = \left(\frac{n_i}{\tilde{C}}\right)^{\frac{1}{2}} \tag{3.16}$$

Both parameters depend on the length of the device and the maximum doping concentration $\tilde{C}$. For typical problems σ ranges from 10^{-3} to 10^{-6}, λ from 10^{-3} to 10^{-7}. For small devices and highly doped semiconductors λ tends to zero acting as a singular perturbation parameter. The corresponding singular perturbation analysis is carried out in Section 3.4.

The form of (3.13) suggests the time scaling

$$t = \frac{L^2}{U_T \tilde{\mu}} t_s, \tag{3.17}$$

where t is the unscaled and t_s denotes the scaled time variable.

For the sake of of legibility the subscript s is omitted below. The scaled drift-diffusion equations (3.13) are then given by:

$$\lambda^2 \Delta V = n - p - C \tag{3.18a}$$

$$\partial_t n = \operatorname{div} J_n - R \tag{3.18b}$$

$$\partial_t p = -\operatorname{div} J_p - R \tag{3.18c}$$

with J_n and J_p given by (3.13d) and (3.13e), the boundary conditions (3.15) and the initial conditions (3.7).

3.2 The Equilibrium Case

The thermal equilibrium refers to the condition in which the specimen is not subject to external excitations, except a uniform temperature. That is no voltages or electric fields are applied. Under thermal equilibrium conditions, every process is balanced in detail by an opposing process.
A semiconductor device is in thermal equilibrium, if all potentials, which are externally applied to the semiconductor contacts are zero, $U(x) \equiv 0$ and the thermal generation is exactly balanced by recombination, $R \equiv 0$. A solution of the reduced stationary drift diffusion equations:

$$\begin{aligned} \lambda^2 \Delta V &= n - p - C \\ 0 &= \mu_n (\operatorname{grad} n - n \ \operatorname{grad} V) \\ 0 &= \mu_p (\operatorname{grad} p - p \ \operatorname{grad} V) \end{aligned}$$

is given by:

$$n = \sigma^2 e^V \qquad\qquad p = \sigma^2 e^{-V} \tag{3.19}$$

The system then reduces to the Poisson equation

$$\lambda^2 \Delta V = \sigma^2 e^V - \sigma^2 e^{-V} - C \tag{3.20a}$$

$$V(x) = V_{bi}(x) = \ln\left(\frac{1}{2\sigma^2}(C(x) + \sqrt{C(x)^2 + 4\,\sigma^4}\right) \qquad \forall x \in \partial\Omega_D \tag{3.20b}$$

$$\frac{\partial V}{\partial \nu} = 0 \qquad\qquad \forall x \in \partial\Omega_N \tag{3.20c}$$

In practice it is assumed that the process starts at equilibrium. Therefore n_0 and p_0 given by (3.19), with V_0 obtained by solving the Poisson equation (3.20), can be used as initial values for the time-dependent problem.

3.3 Analysis of the Transient DD-model

In this section the most important existence and uniqueness results considering the transient drift-diffusion equations are presented. All presented results refer to the work of Gajewski [11] and Markowich, Ringhofer [18].
In 1985 Gajewski [11] proved existence and uniqueness of global-in-time solutions for the transient drift-diffusion equations. Under the assumption that the doping profile $C \in L^r(\Omega)$ for $d \leq r \leq 6$, where d denotes the dimension of space, it is shown that $(V - V_D, n - n_D, p - p_D) \in W$ where W is defined as follows:

$$
\begin{aligned}
W &= \left\{C([0,T]; W^2_{2,0}) \cap L^2([0,T]; W^2_{r,0}) \cap H^1([0,T]; X)\right\} \times Y \times Y \\
Y &= C([0,T]; L^2) \cap L^2([0,T], X) \cap H^1([0,T], X^*) \\
X &= \left\{v \in W^1_2 \mid v = 0 \text{ on } \partial\Omega_D\right\}
\end{aligned}
$$

We consider the following assumptions:

(A1) $\Omega = [0,1]$;

(A2) The doping profile $C \in L^r(\Omega)$;

(A3) The mobilities $\mu_n \in L^\infty(\Omega), \mu_p \in L^\infty(\Omega)$;

Note that in the case of spatial dimension one, which we are interested in, assumption (A1) can be achieved by appropriate spatial scaling. Using the Shockley-Read-Hall recombination-generation rate and assuming that $\tau_n, \tau_p \in L^\infty(\Omega)$ one can show that

$$R_{SRH} = \frac{np - n_i^2}{\tau_p(n + n_i) + \tau_n(p + n_i)} \tag{3.21}$$

is in $C([0,T], L^2(\Omega))$.
For the special case of spatial dimension one we are able to show higher regularity of (V, n, p), which is used in later sections.

Proposition 3.1. Under the assumptions (A1)-(A3) every solution
$(V - V_D, n - n_D, p - p_D) \in W$ satisfies
$(V, n, p) \in C([0,T], H^2(\Omega)) \times C([0,T], W^1_\infty(\Omega))^2$.

Proof. From the Poisson equation it can be shown that

$$\lambda^2 \underset{\in C([0,T],L^2(\Omega))}{\mathrm{V_{xx}}} = \underbrace{\underset{\in C([0,T],L^2(\Omega))}{\mathrm{n}} - \underset{\in C([0,T],L^2(\Omega))}{\mathrm{p}} - \underset{\in L^2(\Omega)}{\mathrm{C}}}_{\in\, C([0,T],L^2(\Omega))}$$

therefore $V \in C([0,T], H^2(\Omega))$. In the case of spatial dimension one, the compact embedding $H^2(\Omega) \hookrightarrow C_b^1(\Omega)$ holds, which denotes the space of continuous bounded functions with continuous and bounded derivative. From the drift-diffusion equations one obtains that

$$n_t - \mu_n n_{xx} = \underbrace{\mu_n(-\underset{\in C([0,T],L^\infty(\Omega))}{\mathrm{n}}\ \underset{\in C([0,T],L^2(\Omega))}{\mathrm{V_{xx}}} - \underset{\in C([0,T],L^2(\Omega))}{\mathrm{n_x}}\ \underset{\in C([0,T],L^\infty(\Omega))}{\mathrm{V_x}}) - \underset{\in C([0,T],L^2(\Omega))}{\mathrm{R}}}_{\in C([0,T],L^2(\Omega))} \tag{3.22}$$

$$p_t - \mu_p p_{xx} = \underbrace{\mu_p(\underset{\in C([0,T],L^\infty(\Omega))}{\mathrm{p}}\ \underset{\in C([0,T],L^2(\Omega))}{\mathrm{V_{xx}}} + \underset{\in C([0,T],L^2(\Omega))}{\mathrm{p_x}}\ \underset{\in C([0,T],L^\infty(\Omega))}{\mathrm{V_x}}) - \underset{\in C([0,T],L^2(\Omega)}{\mathrm{R}}}_{\in C([0,T],L^2(\Omega))} \tag{3.23}$$

Under the following assumptions

1) $(n_I(x), p_I(x), V_I(x)) \in W_\infty^1(\Omega)^3$

2) $(n_D(t), p_D(t), V_D(t)) \in C^1([0,T])^3$

3) The right hand side F_n of (3.22) and F_p of (3.23) is continuous and bounded

Cannon [6] proofed that a unique solution of (3.22) and (3.23) exists. Furthermore the solution is bounded and has a bounded continuous derivative, which is equivalent to $(n,p) \in C([0,T], W_\infty^1(\Omega))^2$.
The initial solution $(V_I(x), n_I(x), p_I(x))$ is obtained by the solution V_0 of the DD-model in thermal equilibrium given by

$$\lambda^2 \frac{\partial^2 V_0}{\partial x^2} = \sigma^2\, e^{V_0} - \sigma^2\, e^{-V_0} - C(x).$$

In [16] it is proved that the drift-diffusion equations in thermal equilibrium have a locally unique solution V_0 in $H^2(\Omega)$, therefore $(n_I(x), p_I(x), V_I(x)) \in H^2(\Omega)$. All other assumptions hold which implies
$(V, n, p) \in C([0,T], H^2(\Omega)) \times C([0,T], W^1_\infty(\Omega))^2$. □

The operator Q maps the applied voltage U to the solution (V, n, p) of the drift-diffusion equations. In the next chapter we will need the continuity and Fréchet differentiability of this operator. Therefore we will show the following result:

Proposition 3.2. The operator

$$\begin{aligned} Q : L^2([0,T], H^{\frac{1}{2}}(\Gamma_2)) &\mapsto C([0,T], H^2(\Omega)) \times C([0,T], W^1_\infty(\Omega))^2 \\ U &\mapsto (V, n, p) \end{aligned}$$

where (V, n, p) are the solution of the drift-diffusion equations given by (3.18), is well-defined and two times Fréchet differentiable. The first derivative at U in a direction ϕ is given by the solution $(\hat{V}, \hat{n}, \hat{p})$ of the partial differential equation system:

$$\lambda^2 \Delta \hat{V} = \hat{n} - \hat{p} \tag{3.24a}$$

$$\frac{\partial \hat{n}}{\partial t} = \operatorname{div}\left(\mu_n \left(\nabla \hat{n} - \hat{n}\nabla V - n\nabla \hat{V}\right)\right) - \hat{R} \tag{3.24b}$$

$$\frac{\partial \hat{p}}{\partial t} = \operatorname{div}\left(\mu_p \left(\nabla \hat{p} + \hat{p}\nabla V + p\nabla \hat{V}\right)\right) - \hat{R} \tag{3.24c}$$

where (V, n, p) denote the solution of the drift-diffusion equations at $U = U(x,t)$. The corresponding boundary conditions are homogeneous Neumann and initial conditions and the Dirichlet boundary conditions $\partial\Omega_D$:

$$\hat{V} = \phi \quad \hat{n} = \hat{p} = 0$$

The second derivative at U in directions (ϕ, ψ) is obtained by the solution $(\bar{V}, \bar{n}, \bar{p})$ of the system

$$\lambda^2 \Delta \bar{V} = \bar{n} - \bar{p} \tag{3.25a}$$

$$\frac{\partial \bar{n}}{\partial t} = \operatorname{div}\left(\mu_n \left(\nabla \bar{n} - \bar{n}\nabla V - n\nabla \bar{V}\right)\right) - \bar{R} \tag{3.25b}$$

$$\frac{\partial \bar{p}}{\partial t} = \operatorname{div}\left(\mu_p \left(\nabla \bar{p} + \bar{p}\nabla V + p\nabla \bar{V}\right)\right) - \bar{R} \tag{3.25c}$$

where (V, n, p) denotes the solution of the drift-diffusion equations at $U = U(x, t)$. Again one has homogeneous initial and Neumann boundary conditions and the Dirichlet boundary conditions are on $\partial\Omega_D$:

$$\bar{V} = \phi\psi \quad \bar{n} = \bar{p} = 0$$

Proof. The operator $Q'(U)$, mapping the applied potential to $(\hat{V}, \hat{n}, \hat{p})$ is linear. For the derivative at $U = U(x, t)$ one obtains that

$$\begin{aligned}
&Q(U + t\phi) - Q(U) - Q'(U)\phi = \\
&\begin{pmatrix} \lambda^2 V_\phi - n_\phi + p_\phi + C \\ \frac{\partial n_\phi}{\partial t} - \operatorname{div}\left(\mu_n\left(\nabla n_\phi - n_\phi \nabla V_\phi\right)\right) \\ \frac{\partial p_\phi}{\partial t} - \operatorname{div}\left(\mu_p\left(\nabla p_\phi + p_\phi \nabla V_\phi\right)\right) \end{pmatrix} - \begin{pmatrix} \lambda^2 V - n + p + C \\ \frac{\partial n}{\partial t} - \operatorname{div}\left(\mu_n\left(\nabla n - n\nabla V\right)\right) \\ \frac{\partial p}{\partial t} - - \operatorname{div}\left(\mu_p\left(\nabla p + p\nabla V\right)\right) \end{pmatrix} - \\
&- \begin{pmatrix} \lambda^2 \hat{V} - \hat{n} + \hat{p} \\ \frac{\partial \hat{n}}{\partial t} - \operatorname{div}\left(\mu_n\left(\nabla \hat{n} - \hat{n}\nabla V - n\nabla \hat{V}\right)\right) \\ \frac{\partial \hat{p}}{\partial t} - \operatorname{div}\left(\mu_p\left(\nabla \hat{p} + \hat{p}\nabla V + p\nabla \hat{V}\right)\right) \end{pmatrix}
\end{aligned}$$

Setting

$$\hat{n} = n_\phi - n \quad \hat{p} = p_\phi - p \quad \hat{V} = V_\phi - V$$

it can be shown that

$$Q(U + t\phi) - Q(U) - Q'(U)\phi = \begin{pmatrix} 0 \\ \operatorname{div}\left(\mu_n\left(\left(n_\phi - n\right)\nabla\left(V_\phi - V\right)\right)\right) \\ \operatorname{div}\left(\mu_p\left(\left(p_\phi - p\right)\nabla\left(V_\phi - V\right)\right)\right) \end{pmatrix}$$

which tends to zero as $t \to 0$.
The continuity of the operator $Q'(U)$ can be shown similarly. $Q'(U)$ is a linear continuous operator and therefore the Fréchet derivative of Q with respect to the applied potential U. Analogous results can be shown for the second Fréchet derivative $Q''(U)$. □

Furthermore Markowich and Ringhofer proved in [18] that the linearization of the DDE given by (3.24) is a strongly continuous semigroup.

Definition 3.3.1. A strongly continuous semigroup is a family $T_t : X \mapsto X, t \geq 0$, of continuous linear operators with the following properties:

1) $T_0 = Is$

2) $T_{s+t} = T_s T_t \quad \forall\, s, t \geq 0$,

3) $\lim_{t \to 0} T_t x = x \quad \forall\, x \in X$

This ensures the stability of the implicit Euler time discretization. Furthermore it is proved that the linearized equation system given by (3.24) is invertible.

3.4 Singular Perturbation Analysis

For highly doped semiconductors the parameter λ given by (3.16) will become very small. For instance, if $L = 10^{-4}$ cm and $\tilde{C} = 10^{21}$ cm^{-3}, λ is of order 10^{-4}. If the size of ΔV is small, the right hand side of (3.18) will be $O(\lambda^2)$. In small regions, so called layers, V has a steep gradient and the left hand side of (3.18) is not vanishing. It is reasonable to assume that away from these layers the solution of the reduced system ($\lambda = 0$) is a good approximation of the solution of the system, while within these layers the whole DD-model has to be considered.
In this section we carry out an asymptotic expansion for a one dimensional unipolar and bipolar semiconductor device. Unipolar devices consist only of n-regions, for example n^+nn^+ diodes. The presented singular perturbation analysis was introduced by Markowich and Ringhofer in [18], where they proved that the composite expansion is an asymptotic evaluation of the solution of the drift-diffusion equations.

Unipolar Semiconductor Device 1D

The unipolar drift-diffusion equations arise from the original DD-system by setting $p \equiv 0$ in Ω. Therefore we obtain

$$\lambda^2 \frac{\partial^2 V}{\partial x^2} = n - C \tag{3.26a}$$

$$\frac{\partial n}{\partial t} = \frac{\partial}{\partial x}\left(\mu_n \left(\frac{\partial n}{\partial x} - n\,\frac{\partial V}{\partial x}\right)\right) \tag{3.26b}$$

$$n(x,t) = n_D(x) = \frac{1}{2}(C(x) + \sqrt{C(x)^2 + 4\,\sigma^4}) \tag{3.26c}$$

$$V(x,t) = V_{bi}(x) + U(x,t) \tag{3.26d}$$

$$n(x,0) = n^I(x) \tag{3.26e}$$

The reduced drift diffusion equations, obtained by setting λ to zero are:

$$0 = n - C \tag{3.27a}$$

$$\partial_t n = \frac{\partial}{\partial x}\left(\mu_n \left(\frac{\partial n}{\partial x} - n\,\frac{\partial V}{\partial x}\right)\right) \tag{3.27b}$$

The doping profile $C(x)$ is time independent, so (3.27) can be simplified to the ordinary differential equation

$$0 = n - C \tag{3.28a}$$

$$0 = \frac{\partial}{\partial x}\left(\frac{\partial C}{\partial x} - C\frac{\partial V}{\partial x}\right) \tag{3.28b}$$

which can be solved analytically. The solution is given by:

$$\bar{n} = C \tag{3.29a}$$

$$\bar{V} = \frac{(\frac{c_1}{\mu_n} - \frac{\partial C}{\partial x})}{C} \cdot x + c_2 \tag{3.29b}$$

with $c_1, c_2 =$ const. We will refer to $(\bar{n}, \bar{V})$ as the outer or reduced solution. The reduced system does not satisfy the boundary conditions of the original system (3.26) and around the n-junction the assumption, that ΔV is small does not hold. Therefore three layers are defined at:

1) $x \in [0, \lambda]$

Figure 3.1: Layer terms of a unipolar Diode

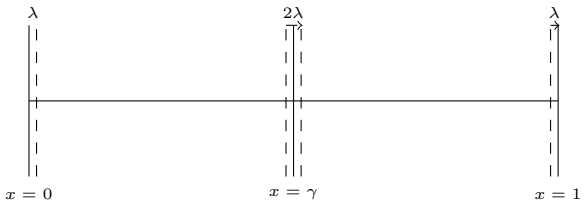

2) $x \in [\gamma - \lambda, \gamma + \lambda]$

3) $x \in [1 - \lambda, 1]$

which can be seen in Figure 3.1. Within these three layers a local coordinate transformation is performed

$$x = X + \lambda\xi$$

where X is a point of the layer (in our case $X \in \{0, \gamma, 1\}$) and $\xi \in \mathbb{R}$. Applying this coordinate transformation to (3.27) and letting λ tend to zero one obtains:

$$\frac{\partial^2 \hat{V}}{\partial \xi^2} = \hat{n} - C_{\underline{+}} \tag{3.30a}$$

$$0 = \frac{\partial}{\partial \xi}(\mu_n(\frac{\partial \hat{n}}{\partial \xi} - \hat{n}\frac{\partial \hat{V}}{\partial \xi})) \tag{3.30b}$$

with $(\hat{n}, \hat{V})$ called the inner solution and the boundary conditions given in (3.26). $f_{\underline{+}}$ denotes the appropriate one sided limit of the function f at the junction. After integration the system reduces to:

$$\frac{\partial^2 \hat{V}}{\partial \xi^2} = \hat{n} - C_{\underline{+}} \tag{3.31a}$$

$$\hat{n} = A_n e^{\hat{V}(\xi,t)} \tag{3.31b}$$

where A_n is given by:

$$A_n = \bar{n}(X,t)e^{\bar{V}(X,t)} \tag{3.32a}$$

and continuous interface conditions.

PN Diode 1D

Looking at bipolar semiconductor devices one obtains similar results as for unipolar devices but there are two major differences. Applying the same transformation to the bipolar semiconductor device one would obtain following equations. The inner solution $(\hat{n}, \hat{p}, \hat{V})$ fulfills the equation system

$$\frac{\partial^2 \hat{V}}{\partial \xi^2} = \hat{n} - \hat{p} - C + O(\lambda) \tag{3.33a}$$

$$O(\lambda) = \frac{\partial \hat{n}}{\partial \xi} - \hat{n}\frac{\partial \hat{V}}{\partial \xi} \tag{3.33b}$$

$$O(\lambda) = \frac{\partial \hat{p}}{\partial \xi} + \hat{p}\frac{\partial \hat{V}}{\partial \xi} \tag{3.33c}$$

Letting λ go to zero and after integration one obtains:

$$\frac{\partial^2 \hat{V}}{\partial \xi^2} = \hat{n} - \hat{p} - C \tag{3.34a}$$

$$\hat{n}(\xi, t) = A_n(\xi, t)e^{\hat{V}(\xi,t)} \tag{3.34b}$$

$$\hat{p}(\xi, t) = A_p(\xi, t)e^{-\hat{V}(\xi,t)} \tag{3.34c}$$

where A_n and A_p are given by

$$A_n = \bar{n}(X, t)e^{-\bar{V}(X,t)}$$

$$A_p = \bar{p}(X, t)e^{\bar{V}(X,t)}$$

and continuous interface conditions.

The outer solution $\left(\bar{n}, \bar{p}, \bar{V}\right)$, obtained by setting $\lambda = 0$ is:

$$0 = \bar{n} - \bar{p} - C \tag{3.35a}$$

$$\frac{\partial \bar{n}}{\partial t} = \frac{\partial}{\partial x}\bar{J}_n - \bar{R} \tag{3.35b}$$

$$\frac{\partial \bar{p}}{\partial t} = -\frac{\partial}{\partial x}\bar{J}_p - \bar{R} \tag{3.35c}$$

$$\bar{J}_n = \mu_n \left(\frac{\partial \bar{n}}{\partial x} - \bar{n}\frac{\partial \bar{V}}{\partial x}\right) \tag{3.35d}$$

$$\bar{J}_p = \mu_p \left(-\frac{\partial \bar{p}}{\partial x} - \bar{p}\frac{\partial \bar{V}}{\partial x}\right) \tag{3.35e}$$

Figure 3.2: Layer terms of a np-Diode

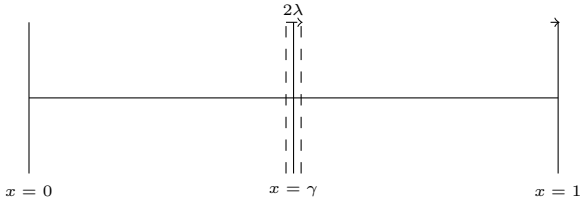

The concentration of the carriers can be expressed by:

$$\bar{n} = \bar{p} + C$$

Assuming that the doping profile C is not time dependent and constant on the domain the system (3.35) reduces to:

$$\begin{aligned} 0 &= \frac{\partial}{\partial x}\left(\bar{J}_n + \bar{J}_p\right) \\ \frac{\partial \bar{p}}{\partial t} &= -\frac{\partial}{\partial x}\bar{J}_p - \bar{R} \\ \bar{J}_n &= \mu_n\left(\frac{\partial \bar{p}}{\partial x} - (\bar{p} + C)\frac{\partial \bar{V}}{\partial x}\right) \\ \bar{J}_p &= -\mu_p\left(\frac{\partial \bar{p}}{\partial x} - \bar{p}\frac{\partial \bar{V}}{\partial x}\right) \end{aligned}$$

The Dirichlet boundary conditions hold, just a single layer term has to be added at the pn-junction, see Figure 3.2. Furthermore the outer solution is still time dependent so consistent initial values have to be provided.
If one would use the thermal equilibrium solution given by (3.20) as an initial guess the concentration of the carriers at $t = 0$ would be:

$$\bar{n}(x, 0) = \sigma^2 e^{-V_0} + C$$

Inserting this initial guess into (3.35) one gets:

$$\begin{aligned}
&\operatorname{div}\left(\bar{J}_n + \bar{J}_p\right) = \\
&= \operatorname{div}\left(\mu_n\left(-\sigma^2 \operatorname{grad} V_0 e^{-V_0} + \operatorname{grad} C - \sigma^2 e^{-V_0} \operatorname{grad} V_0 - C \operatorname{grad} V_0\right) + \right. \\
&\left. + \mu_p\left(\sigma^2 \operatorname{grad} V_0 e^{-V_0} - \sigma^2 e^{-V_0} \operatorname{grad} V_0\right)\right) = \\
&= \operatorname{div}\left(\mu_n\left(2\sigma^2 \operatorname{grad} V_0 e^{V_0} + \operatorname{grad} C - C \operatorname{grad} V_0\right)\right) \neq 0
\end{aligned}$$

The drift diffusion equations in equilibrium state do not fulfill the reduced equations at $t = 0$. In order to obtain consistent initial values, the steady state drift diffusion equations have to be solved, which are obtained from the transient case by setting

$$\frac{\partial n}{\partial t} = \frac{\partial p}{\partial t} = 0.$$

Therefore instead of solving a single PDE one has to solve a system of partial differential equations, which increases the numerical effort significantly. For further information on the asymptotic behavior of the transient DD-model we refer to [19].

Chapter 4

Inverse Dopant Profiling

The inverse doping problem corresponds to the problem of identifying the doping profile $C(x)$ in system (3.18) from indirect measurements. The following types of measurements are used in practice:

1. Current measurements
   The current flow through a contact $\Gamma_1 \subset \partial\Omega_D$:
   $$I_{\Gamma_1}(U) = \int_{\Gamma_1} (J_n + J_p) \cdot \nu \, ds \tag{4.1}$$

2. Capacitance measurements
   The mean capacitance at a contact $\Gamma_1 \subset \partial\Omega_D$:
   $$Cap_{\Gamma_1}(U) = \frac{d}{dU} \left(\int_{\Gamma_1} \frac{\partial V}{\partial \nu} \, ds \right) \tag{4.2}$$

In all cases we assume that $\Gamma_1 \subset \partial\Omega_D$ is sufficiently regular with a non zero measure. Another possibility to obtain indirect measurements is the so called laser-beam-inducted current (LBIC) technique. The inverse problem of reconstructing the doping profile form LBIC measurements was considered in [2] and [9].
In the next subsections we investigate whether the operators, which map the applied potential U to the current or capacitance measurements, are well-defined and continuous in appropriate spaces.

The Current-Voltage Map

The voltage current data are the measurements of the normal component of the current density J on a contact $\Gamma_1 \subset \partial\Omega_D$ for an applied time dependent voltage $U(x,t)$. The current-voltage map is given by:

$$\begin{aligned} \Sigma_C : L^2([0,T], H^{\frac{1}{2}}(\Gamma_2)) &\to L^2([0,T], H^{\frac{1}{2}}(\Gamma_1)) \\ U &\mapsto \int_{\Gamma_1} J \cdot \nu \, ds = \int_{\Gamma_1} (J_n + J_p) \cdot \nu \, ds \end{aligned} \tag{4.3}$$

where $\Gamma_2 \subset \partial\Omega_D$ and $\Gamma_1 \cap \Gamma_2 = \emptyset$. The non-linear operator Σ_C is well-defined, continuous and Fréchet-differentiable between suitable Sobolev Spaces therefore the following proposition holds.

Proposition 4.1. For each applied voltage $U \in L^2([0,T], H^{\frac{1}{2}}(\Gamma_2))$ the operator given by (4.3) is well-defined, continuous and Fréchet differentiable.

Proof. In Section 3.3 we showed that for the every U a unique solution $(V,n,p) \in C([0,T], H^2(\Omega)) \times C([0,T], W^1_\infty(\Omega))^2$ exists. Therefore the current flow $J \cdot \nu$ over a contact Γ_1 is well-defined. The operator Σ_C can be written as:

$$\Sigma_C = \Sigma_C^1 \circ \Sigma_C^2 \tag{4.4}$$

$$\Sigma_C^1 : (V,n,p) \to \int_{\Gamma_1} J \cdot \nu \, ds \tag{4.5}$$

$$\Sigma_C^2 : U \to (V,n,p) \tag{4.6}$$

The derivative in direction ϕ of the drift diffusion equations (3.18) with respect to U is given by (3.24). The mapping Σ_C^2 is linear and continuous - for details see Section 3.3. Therefore Σ_C^2 maps the applied voltage continuously to the solution $(V,n,p) \in C([0,T], H^2(\Omega)) \times C([0,T], W^1_\infty(\Omega))^2$ of the DD-model.
The Fréchet derivative of Σ_C^1 at (V,n,p) in the direction (V',n',p') is given by

$$\begin{aligned} \left(\Sigma_C^1\right)'(V,n,p) = \int_{\Gamma_1} \Bigg[&\mu_n \left(\frac{\partial n'}{\partial \nu} - n \frac{\partial V'}{\partial \nu} - n' \frac{\partial V}{\partial \nu} \right) - \\ &- \mu_p \left(\frac{\partial p'}{\partial \nu} + p \frac{\partial V'}{\partial \nu} + p' \frac{\partial V}{\partial \nu} \right) \Bigg] \, ds \end{aligned} \tag{4.7}$$

$(\Sigma_C^1)'$ is a linear continuous operator. Therefore Σ_C given by (4.3) is well-defined, continuous and Fréchet-differentiable. □

Capacitance Measurements

Capacitance measurements are the variation of the electric flux in normal direction on a contact Γ_1 with respect to the applied voltage U. The corresponding operator is

$$T_C : L^2([0,T], H^{\frac{1}{2}}(\Gamma_2)) \to L^2([0,T], H^{\frac{1}{2}}(\Gamma_1)) \tag{4.8}$$
$$U \mapsto \int_{\Gamma_1} \frac{\partial \hat{V}}{\partial \nu}\, ds$$

where $\hat{V}$ is the solution of the linearized drift-diffusion equations at equilibrium, i.e. $U \equiv 0$

$$\lambda^2 \Delta \hat{V} = \hat{n} - \hat{p} \tag{4.9a}$$
$$\frac{\partial \hat{n}}{\partial t} = \operatorname{div}\left(\mu_n \left(\nabla \hat{n} - \sigma^2\, e^{V_0}\, \nabla \hat{V} - \hat{n}\, \nabla V_0\right)\right) \tag{4.9b}$$
$$\frac{\partial \hat{p}}{\partial t} = \operatorname{div}\left(\mu_p \left(\nabla \hat{p} + \sigma^2\, e^{-V_0}\, \nabla \hat{V} + \hat{p}\, \nabla V_0\right)\right) \tag{4.9c}$$

with homogeneous initial conditions, homogeneous Neumann boundary conditions and the Dirichlet boundary conditions on $\partial\Omega_D$

$$\hat{V} = \phi, \quad \hat{n} = \hat{p} = 0$$

V_0 denotes the solution of the Poisson equation in thermal equilibrium given by (3.20).

Proposition 4.2. For each applied voltage U the operator given by (4.8) is well-defined, continuous and Fréchet-differentiable.

Proof. The operator T_C can be written as:

$$T_C = T_C^1 \circ T_C^2 \tag{4.10}$$
$$T_C^1 : (\hat{n}, \hat{p}, \hat{V}) \mapsto \int_{\Gamma_1} \frac{\partial V}{\partial \nu}\, ds \tag{4.11}$$
$$T_C^2 : U \mapsto (\hat{n}, \hat{p}, \hat{V}) \tag{4.12}$$

T_C^1 is obviously continuous and Fréchet differentiable. The operator T_C^2 maps the applied potential to the solution of the linearized equations (3.24) at $U = 0$. In

Section 3.3 it has been shown that T_C^2 is a linear continuous mapping, which has a continuous Fréchet derivative. Therefore T_C is a well-defined, continuous and Fréchet-differentiable operator. □

4.1 Identification of the Doping profile

In this section the identification of the doping profile either from voltage-current data or capacitance measurements is discussed.

Identification from Voltage-Current Data

The abstract formulation of the identification problem using current measurements is given by:

$$F(C) = Y^\delta \tag{4.13}$$

with

$$F\colon D(F) \subset \mathcal{X} \mapsto \mathcal{Y} \tag{4.14}$$

and

$$\mathcal{X} = L^2(\Omega)$$
$$\mathcal{Y} = \Sigma_C(U)$$

The domain of the operator F is:

$$D(F) = \left\{C \in H^1(\Omega) \mid \underline{C} \leq C(x) \leq \overline{C}, \text{ a.e. in } \Omega\right\}$$

with $\underline{C}, \overline{C} = \text{const} > 0$.
Y^δ represents the noisy current data, which is assumed to be bounded by δ:

$$\left\|Y^\delta - Y\right\| \leq \delta$$

With these assumptions one can show the following results

Proposition 4.3. The map

$$\begin{aligned} F\colon D(F) \subset \mathcal{X} &\to \mathcal{Y} \\ C &\mapsto \Sigma_C(U) \end{aligned}$$

is well-defined, continuous and Fréchet-differentiable in $\mathcal{X}$. Furthermore the operator F is weakly sequentially closed.

Proof. The operator F can be written as:

$$\begin{aligned} F &= F_1 \circ F_2 \\ F_2 &: C \to (n, p, V) \\ F_1 &: (n, p, V) \to J \cdot \nu \end{aligned}$$

F_1 equals the operator Σ_C^1 given by (4.5), which is continuous and Fréchet differentiable. It remains to show that the operator F_2 is continuous and differentiable. The drift-diffusion equations (3.18) can be written as

$$E(n, p, V) = \begin{pmatrix} C \\ 0 \\ 0 \end{pmatrix}$$

$$E(n, p, V) = \begin{pmatrix} \lambda^2 \Delta V - n + p \\ \frac{\partial n}{\partial t} - \operatorname{div} J_n + R \\ \frac{\partial p}{\partial t} + \operatorname{div} J_p + R \end{pmatrix}$$

Differentiation gives:

$$E'(n, p, V) \begin{pmatrix} n' \\ p' \\ V' \end{pmatrix} = \begin{pmatrix} C' \\ 0 \\ 0 \end{pmatrix}$$

In [18] it is shown that $E'(n, p, V)$ is a strongly continuous semigroup and invertible. Therefore we can rewrite the problem as

$$F_2'(C)(C') = \begin{pmatrix} n' \\ p' \\ V' \end{pmatrix} = E'(n, p, V)^{-1} \begin{pmatrix} C' \\ 0 \\ 0 \end{pmatrix}$$

Using the chain rule the derivative of F is given by

$$F' = F_1'(F_2) \circ F_2'$$

The derivatives of F_1 and F_2 are continuous and Fréchet differentiable, thus F is continuous and Fréchet differentiable.
It is still left to show that F is weakly sequentially closed, i.e., for any sequence $\{C_n\} \subset D(F)$, weak convergence of C_n to $C \in \mathcal{X}$ and weak convergence of $F(C_n)$ to $y \in \mathcal{Y}$ imply that $C \in D(F)$ and $F(C) = y$.
In case of spatial dimension one the embedding

$$H^1(\Omega) \hookrightarrow L^\infty(\Omega)$$

is compact, which implies that from $C_n \in D(F)$ we have uniform boundedness of the sequence $\{C_n\} \in L^\infty(\Omega)$ and therefore a weakly* convergent subsequence exists. The uniqueness of the limit implies $C \in L^\infty(\Omega) \cap D(F)$.
$F : X \to \mathcal{Y}$ is continuous so

$$F(C_n) \to F(C) \text{ and } F(C_n) \to y$$

Therefore $C \in D(F)$ and $F(C) = y$. □

Identification from Capacitance Measurements

Similar to the case of current-voltage data the identification problem can be written in the abstract form

$$F(C) = Y^\delta \tag{4.15}$$

with

$$F\colon D(F) \subset \mathcal{X} \mapsto \mathcal{Y} \tag{4.16}$$

and

$$\mathcal{X} = L^2(\Omega)$$
$$\mathcal{Y} = T_C(U)$$

The domain of the operator F is the same as in the case of V-C map.

Proposition 4.4. The map

$$\begin{aligned} F\colon D(F) \subset \mathcal{X} &\to \mathcal{Y} \\ C &\mapsto T_C(U) \end{aligned}$$

is well-defined, continuous and Fréchet-differentiable in $\mathcal{X}$. Furthermore the operator F is weakly sequentially closed.

Proof. The operator F can be written as:

$$\begin{aligned} F &= F^2 \circ F^1 \\ F^1 &: C \mapsto (\hat{n}, \hat{p}, \hat{V}) \\ F^2 &: (\hat{n}, \hat{p}, \hat{V}) \mapsto \frac{\partial V}{\partial \nu} \end{aligned}$$

The operator F_1 can be written as

$$\begin{aligned} F^1 &= F_1^1 \circ F_2^1 \\ F_1^1 &= C \mapsto (n, p, V) \\ F_2^1 &= (n, p, V) \mapsto (\hat{n}, \hat{p}, \hat{V}) \end{aligned}$$

In the proof of Proposition (4.1) we have seen that the operator F_1^1 is continuous and Fréchet differentiable. It can easily be shown that the operator F_2^1 is continuous. F_2^1 is linear with respect (V, n, p), therefore F^1 is continuous and differentiable.
F_2 is linear, continuous and Fréchet differentiable. This implies that F is a linear, continuous and Fréchet differentiable operator.
Using the same arguments as in the proof of Proposition (4.1) one can show that F is weakly sequentially closed. □

4.2 Regularization Methods

In this section regularization methods are discussed, which allow a stable solution of the inverse doping problem. Because of the ill-posedness and the noise in the data caused by measurement errors, standard iterative methods cannot be used to solve equation (4.13) in a stable way.
The exact data shall be denoted by Y the noisy one by Y^δ and we assume that the error is bounded by

$$\left\|Y - Y^\delta\right\| \leq \delta$$

In the case of current measurements one obtains

$$\int_0^T \left|I_{\Gamma_1}(U) - f(t)\right|^2 \, dt \leq \delta$$

where $f(t)$ denotes the current measured on $\Gamma_1 \subset \partial\Omega_D$. Using capacitance measurements the assumptions is given by

$$\int_0^T \left|Cap_{\Gamma_1}(U) - q(t)\right|^2 \, dt \leq \delta$$

where $q(t)$ is the capacitance measured on $\Gamma_1 \subset \partial\Omega_D$.

Tikhonov Regularization

Using Tikhonov regularization equation (4.13) is replaced by the minimization problem:

$$Q(u, C) = \left\|F(C) - Y^\delta\right\|^2 + \alpha \left\|C - C^*\right\|^2 \to \min_{C \in D(F)} \tag{4.17}$$

where $\alpha > 0$, C^* is a starting value and $u = (V, n, p, V_0)$. α is referred to as the regularization parameter. Several rules to choose α accurately can be found in literature. We determine $\alpha(\delta)$ according to the Morozov's discrepancy principle, i.e.

$$\left\|F\left(C_\alpha^\delta\right) - Y^\delta\right\| = \delta \tag{4.18}$$

where C_α^δ is the regularized solution, which depends on the regularization parameter α and on the noise level δ.

Under the assumptions that F is continuous and weakly sequentially closed it can be shown that the minimization problem (4.17) admits a solution, which will not be unique in general. Furthermore the problem of solving (4.17) is stable, this means that the solution depends continuously on the perturbed data Y^δ. For the convergence analysis we refer to [8].

Total Variation Regularization

Another Tikhonov-type regularization method uses the total variation of a function. This approach was originally introduced by Rudin, Osher and Fatemi [20], for further information we also refer to [7] and [1]. Total variation regularization was originally used in image restoration, because discontinuities in the solution were preserved. The total variation functional is defined by:

$$J_0(u) := \sup_{v \in V} \int_\Omega u \operatorname{div} v \, dx \tag{4.19}$$

where the set of test functions is given by

$$V = \left\{ v \in C_0^\infty(\Omega)^d \mid \|g\|_\infty \leq 1 \right\}$$

If $u \in C^1(\Omega)$ one can show, using integration by parts that

$$J_0(u) = \int_\Omega |\nabla u| \, dx$$

The space of functions of bounded variation $BV(\Omega)$ is defined as:

$$BV(\Omega) = \left\{ u \in L^1(\Omega) \mid J_0(u) < \infty \right\}$$

The total variation functional (4.19) is a seminorm, the BV norm is given by:

$$\|u\|_{BV} = \|u\|_{L^1(\Omega)} + J_0(u)$$

With respect to this norm $BV(\Omega)$ is a Banach space. The seminorm $J_0(u)$ is not differentiable in $\nabla u = 0$ therefore one often considers a slightly different functional

$$J_\beta(u) = \int_\Omega \sqrt{|\nabla u|^2 + \beta} \, dx$$

where $\beta \geq 0$. The derivative of $J_\beta(u)$ in direction v is given by

$$J'_\beta(u)v = \int_\Omega \frac{\nabla u \nabla v}{\sqrt{|\nabla u|^2 + \beta}}\, dx$$

The corresponding regularized minimization problem is given by:

$$Q(u, C) = \left\|F(C) - Y^\delta\right\|^2 + \alpha J_\beta(C) \to \min_{C \in D(F)} \tag{4.20}$$

where α denotes the regularization parameter, determined by the discrepancy principle (4.18). In [1] is shown that a unique solution of the minimization problem (4.20) exists if Q is weakly lower semicontinuous and BV-coercive.

Definition 4.2.1. A functional Q is

(a) BV-coercive if

$$\|C\|_{BV} \to +\infty \quad \Rightarrow \quad Q(C) \to +\infty$$

(b) weakly lower semicontinuous if

$$C_n \rightharpoonup C,\ f(C_n) \leq c \quad \Rightarrow \quad f(C) \leq c$$

We are able to show that the minimization functional (4.20) is weakly lower semicontinuous and BV-coercive, which implies the existence of a unique minimizer.

Proposition 4.5. The minimization functional (4.20) is weakly lower semicontinuous and BV-coercive.

Proof. In [1] it is shown that the functional $J_\beta(C)$ is weakly lower continuous for any $\beta \geq 0$. In Proposition 4.3 it has been proved that F is continuous in $L^2(\Omega)$, which implies the weak lower semicontinuity of F. Therefore the functional Q is weakly lower semicontiuous.
Furthermore

$$Q(C) = \left\|F(C) - Y^\delta\right\|^2 + \alpha J_\beta(C) \geq \alpha \|C\|_{BV}$$

and Q(C) tends to infinity if $\|C\|_{BV} \to \infty$. □

Iterative Regularization Methods

The simplest iterative regularization method is the Landweber iteration

$$C_{k+1} = C_k - \omega F'(C_k)(F(C_k) - Y^\delta) \tag{4.21}$$

with an appropriate damping parameter $\omega \in \mathbb{R}^+$. This method is a stable fixed point method and rather slow. A faster iterative method is the Levenberg Marquardt iteration:

$$C_{k+1} = C_k - \left(F'(C_k)^* F'(C_k) + \alpha_k\, I\right)^{-1} F'(C_k)^* \left(F(C_k) - Y^\delta\right) \tag{4.22}$$

where I denotes the identity operator and F^* the adjoint operator.
The main disadvantage of iterative regularization methods is the high effort in each iteration step. The evaluation of the operator F already requires the solution of a non-linear partial differential equation system. Therefore the evaluation of the adjoint operator and its derivatives would be very time consuming. For more information on iterative regularization methods we refer to [8].
In the remainder of this section Tikhonov type regularization with an appropriate initial guess C^* will be considered.

4.3 Gradient Based Optimization

In this section we will briefly discuss gradient based optimization algorithms to minimize the functional (4.17) or (4.20). In the last sections we proved that both functionals have a unique minimizer and that all introduced operators are Fréchet differentiable. Therefore one can use gradient based methods for minimization, which are given by

$$C_{k+1} = C_k - \tau \tilde{Q}'(C_k) \tag{4.23}$$

with $\tau \in \mathbb{R}^+$ determined by step-size control and $\tilde{Q}(C) = Q(u(C), C)$.
In literature several different optimization methods based on gradient evaluation are defined. The two most basic algorithms are the steepest descent and the BFGS method, which will be introduced in the next paragraphs.

Both methods are based on line search which creates the iterates by

$$C_{k+1} = C_k + \alpha_k p_k$$

where p_k is the search direction and $\alpha_k > 0$. Here a line search is employed along the search direction p_k. Line searches are distinguished between exact and inexact procedures, depending on what method for calculating the step size is employed. An exact procedure performs a one dimensional line minimization along the search direction p_k to find a step length α_k. Therefore α is iteratively changed until it is minimal along the search direction. Computationally less demanding are inexact line searches, which change α iteratively such that a sufficiently decreasing condition is satisfied.

Many inexact line search methods have been proposed: Goldstein, Armijo, Wolfe, Powell and others. For details we refer to [10] and [13]. Throughout this paper Wolfe-Powell restrictions have been used, which are given by

$$F(C_k + \alpha_k p_k) - F(C_k) \leq \mu_1 \, \alpha_k \, F'(C_k) \, p_k$$
$$F'(C_k + \alpha_k p_k)^* p_k > \sigma F'(C_k)^* p_k$$

with $0 < \mu_1 < 1$ and $\mu_1 < \sigma < 1$. Depending on the choice of the search direction p_k two of the most common methods are:

(1) **Steepest Decent Algorithm:**

The steepest descent algorithm is the simplest and oldest line search method. The search direction is taken as the negative gradient of the objective function, therefore $p_k = -\tilde{Q}'(C_k)$.

The main disadvantage is the very slow linear convergence rate, but one has global convergence.

(2) **Quasi-Newton methods:**

The iterations of Quasi Newton methods look like:

$$C_{k+1} = C_k + \alpha_k p_k \text{ with } p_k = -B_k \nabla F(C_k)$$

where B_k is a positive definite operator chosen so that the search direction tends to approximate the Newton direction. Well-known methods are the

BFGS (Broyden-Fletcher-Goldfarb-Shanno) method and the DFP (Davidson-Fletcher-Powell) method. The main advantage of Quasi Newton methods is the fast convergence and the absence of second order derivatives. Furthermore update formulas can be used to calculate B_{k+1} from B_k.

Additional information on the underlying analysis and convergence rates can be found in [10] and [13].

4.4 Adjoint Approach

In the following we detail the basic ingredients of the adjoint method used for the computation of sensitivities below. Using gradient based methods such as (4.23) requires the computation of the gradient of Q, which causes high numerical effort. Using the dual or adjoint approach the computational cost is often much cheaper. The Tikhonov functional (4.17) can be rewritten as a constrained minimization problem

$$Q(u(C), C) \to \min_C \quad \text{under} \quad P(u(C), C) = 0 \tag{4.24}$$

This system is characterized by an input C, an output u and one or more restrictions

$$P(u(C), C) = 0$$

We consider the minimization problem (4.17) using current measurements. Therefore $u = (n, p, V, V_0)$ satisfying the transient drift-diffusion equations

$$\begin{aligned}
\lambda^2 \Delta V &= n - p - C \\
\partial_t n &= \operatorname{div} J_n - R \\
\partial_t p &= -\operatorname{div} J_p - R \\
J_n &= \mu_n(\operatorname{grad} n - n \ \operatorname{grad} V) \\
J_p &= \mu_p(-\operatorname{grad} p - p \ \operatorname{grad} V)
\end{aligned}$$

and the drift diffusion model in equilibrium state given by

$$\lambda^2 \Delta V = \sigma^2 e^V - \sigma^2 e^{-V} - C$$

By the chain rule the linearization of Q is given by

$$\frac{dQ}{dC} = \frac{\partial Q}{\partial u}\frac{du}{dC} + \frac{\partial Q}{\partial C} \tag{4.25}$$

subject to the constraint that du/dC solves the linearized equation

$$\frac{\partial P}{\partial C}\frac{du}{dC} + \frac{\partial P}{\partial C} = 0. \tag{4.26}$$

Note that the existence and uniqueness for a solution is guaranteed by Proposition 4.1. By defining

$$v := \frac{du}{dC}, \quad A := \frac{\partial P}{\partial u}$$
$$g := \frac{\partial Q}{\partial u}^*, \quad f := -\frac{dP}{dC}$$

(4.25) can be rewritten as

$$\frac{dQ}{dC} = \langle g, v\rangle + \frac{\partial Q}{\partial C}$$

subject to

$$Av = f.$$

Instead of evaluating $\langle g, v\rangle$ the dual form can be used, evaluating $\langle w, f\rangle$ where the adjoint solution w satisfies the equation

$$A^* w = g.$$

The equivalence of the two forms follows from

$$\langle w, f\rangle = \langle w, Av\rangle = \langle A^* w, v\rangle = \langle g, v\rangle$$

Using the adjoint approach one just has to solve a single linear equation system, instead of solving a linear equation system for every value of C.
The Lagrange functional $\mathcal{L}$ of the constrained minimization problem (4.24) is given by:

$$\mathcal{L}(u, C, \lambda) = Q(u, C) + \langle P(u, C), \lambda\rangle \tag{4.27}$$

The Kuhn-Tucker conditions, which are necessary but not sufficient for a minimum are:

$$\frac{\partial \mathcal{L}}{\partial u}(u, C, \lambda) = \frac{\partial Q}{\partial u}(u, C) + \frac{\partial P^*}{\partial u}(u, C)\,\lambda = 0 \tag{4.28a}$$

$$\frac{\partial \mathcal{L}}{\partial C}(u, C, \lambda) = \frac{\partial Q}{\partial C}(u, C) + \frac{\partial P^*}{\partial C}(u, C)\,\lambda = 0 \tag{4.28b}$$

$$\frac{\partial \mathcal{L}}{\partial \lambda}(u, C, \lambda) = P(u, C) = 0 \tag{4.28c}$$

The Lagrange parameters λ can be easily obtained by rearranging equation (4.28a)

$$\lambda = -(\frac{\partial P^*}{\partial u})^{-1}\frac{\partial Q}{\partial u} \tag{4.29}$$

Inserting (4.29) into (4.28b) in direction h gives:

$$\frac{\partial \mathcal{L}}{\partial C}h = \left\langle \frac{\partial Q}{\partial C}, h \right\rangle - \left\langle \frac{\partial P}{\partial C}, \left(\frac{\partial P^*}{\partial u}\right)^{-1}\frac{\partial Q}{\partial u}h \right\rangle \tag{4.30}$$

Likewise substitution of the partial derivatives du/dC in (4.25) by (4.26) gives:

$$\frac{dQ}{dC}h = \left\langle \frac{\partial Q}{\partial C}, h \right\rangle - \left\langle \frac{\partial Q}{\partial u}, \left(\frac{\partial P}{\partial u}\right)^{-1}\frac{\partial P}{\partial C}h \right\rangle \tag{4.31}$$

Rearranging (4.31) yields:

$$\frac{dQ}{dC}h = \left\langle \frac{\partial Q}{\partial C}, h \right\rangle - \left\langle \left(\frac{\partial P^*}{\partial u}\right)^{-1}\frac{\partial Q}{\partial u}h, \frac{\partial P}{\partial C} \right\rangle$$

Therefore

$$\frac{\partial \mathcal{L}}{\partial C}h = \frac{dQ}{dC}h \quad \forall h \in L^2.$$

Hence, the total derivative $\frac{dQ}{dC}$ can be calculated using the Fréchet derivatives of the corresponding Lagrange functional with respect to C.

4.5 Sensitivities

As we have seen in the previous section that instead of evaluating the gradient of the minimization functional Q we can compute the gradient of the corresponding Lagrange functional $\mathcal{L}$. We take advantage of this fact in the computations.

Voltage Current Measurements

As already mentioned the solution of the DD system in thermal equilibrium given by (3.20) is used as initial conditions for the time-dependent problem (3.18). Therefore the constraints $P(u, C) = 0$ of the minimization problem (4.17) are the drift diffusion equations and the reduced system in equilibrium state given by (3.20). The Dirichlet boundary is divided in two parts (anode and cathode)

$$\partial\Omega_D = \Gamma_1 \cup \Gamma_2 \quad \text{with} \quad \Gamma_1 \cap \Gamma_2 = \emptyset$$

$$\begin{aligned}
\mathcal{L}(\lambda_1,\lambda_2,\lambda_3,\lambda_4,n,p,V,V_0) = &\int_0^T\!\!\int_\Omega \lambda_1\,(\lambda^2\Delta V - n + p + C)\,dx\,dt + \\
&+ \int_0^T\!\!\int_\Omega \lambda_2\,(\frac{\partial n}{\partial t} - \operatorname{div}\mu_n(\nabla n - n\nabla V) + R(n,p))\,dx\,dt + \\
&+ \int_0^T\!\!\int_\Omega \lambda_3\,(\frac{\partial p}{\partial t} - \operatorname{div}\mu_p(\nabla p + p\nabla V) + R(n,p))\,dx\,dt + \\
&+ \int_\Omega \lambda_4\,(\lambda^2\Delta V_0 - \sigma^2 e^{V_0} + \sigma^2 e^{-V_0} + C)\,dx + \\
&+ \int_0^T \Big|\int_{\Gamma_1} (\mu_n(\nabla n - n\nabla V) - \mu_p(\nabla p + p\nabla V))\,\nu\,ds - f(t)\Big|^2\,dt + \\
&+ \alpha\int_\Omega |C - C^*|^2\,dx
\end{aligned} \tag{4.32}$$

where ν denotes the outer normal vector and C^* is an initial guess for the doping profile C . After integration by parts with respect to time one obtains

$$\begin{aligned}
\mathcal{L} = & \int_0^T\!\!\int_\Omega \lambda_1 \left(\lambda^2 \Delta V - n + p + C\right) dx\, dt - \\
& - \int_0^T\!\!\int_\Omega \frac{\partial \lambda_2}{\partial t} n \, dx\, dt + \int_\Omega \lambda_2(x,T)\, n(x,T)\, dx - \int_\Omega \lambda_2(x,0) \overbrace{n(x,0)}^{=\sigma^2 e^{V_0}}\, dx + \\
& + \int_0^T\!\!\int_\Omega \lambda_2 \left(-\operatorname{div} \mu_n(\nabla n - n \nabla V) + R(n,p)\right) dx\, dt - \\
& - \int_0^T\!\!\int_\Omega \frac{\partial \lambda_3}{\partial t} p \, dx\, dt + \int_\Omega \lambda_3(x,T)\, p(x,T)\, dx - \int_\Omega \lambda_3(x,0) \overbrace{p(x,0)}^{=\sigma^2 e^{-V_0}}\, dx + \\
& + \int_0^T\!\!\int_\Omega \lambda_3 \left(-\operatorname{div} \mu_p(\nabla p + p \nabla V) + R(n,p)\right) dx\, dt + \\
& + \int_\Omega \lambda_4 \left(\lambda^2 \Delta V_0 - \sigma^2 e^{V_0} + \sigma^2 e^{-V_0} + C\right) dx + \\
& + \int_0^T \Big| \int_{\Gamma_1} \left(\mu_n \left(\nabla n - n \nabla V\right) - \mu_p \left(\nabla p + p \nabla V\right)\right)\, \nu \, ds - f(t) \Big|^2 \, dt + \\
& + \alpha \int_\Omega |C - C^*|^2 \, dx
\end{aligned}$$

The partial derivative of the Lagrange functional with respect to n in a direction h_n is

$$\begin{aligned}
\frac{\partial \mathcal{L}}{\partial n}\, h_n = & \int_0^T\!\!\int_\Omega (-\lambda_1 - \frac{\partial \lambda_2}{\partial t})\, h_n \, dx\, dt + \int_\Omega \lambda_2(x,T)\, h_n(x,T)\, dx - \\
& - \int_0^T\!\!\int_\Omega \lambda_2 \, \operatorname{div} \mu_n(\nabla h_n - h_n \nabla V)\, dx\, dt + \\
& + \int_0^T\!\!\int_\Omega \lambda_2 \, \frac{\partial R(n,p)}{\partial n} h_n \, dx\, dt + \\
& + \int_0^T\!\!\int_\Omega \lambda_3 \, \frac{\partial R(n,p)}{\partial p}\, h_n \, dx\, dt + \int_0^T \frac{\partial BT}{\partial n} h_n \, dt
\end{aligned}$$

and BT denotes the boundary terms given by

$$BT = \int_0^T \Big| \int_{\Gamma_1} \left(\mu_n \left(\nabla n - n \nabla V\right) - \mu_p \left(\nabla p + p \nabla V\right)\right)\, \nu \, ds - f(t) \Big|^2 \, dt$$

Integration by parts then yields

$$\begin{aligned}\frac{\partial \mathcal{L}}{\partial n}\, h_n = &\int_0^T\!\!\int_\Omega (-\lambda_1 - \frac{\partial \lambda_2}{\partial t})\, h_n\, dx\, dt + \int_\Omega \lambda_2(x,T)\, h_n(x,T)\, dx - \\ &- \int_0^T\!\!\int_\Omega \mu_n\, \Delta\lambda_2\, h_n\, dx\, dt + \int_0^T\!\!\int_{\partial\Omega} \mu_n \nabla\lambda_2\, h_n\, \nu\, ds\, dt - \\ &- \int_0^T\!\!\int_\Omega \mu_n\, \nabla\lambda_2 \nabla V h_n\, dx\, dt - \\ &- \int_0^T\!\!\int_{\partial\Omega} \lambda_2\, \mu_n(\nabla h_n - h_n \nabla V)\, \nu\, ds\, dt + \\ &+ \int_0^T\!\!\int_\Omega (\lambda_2 + \lambda_3)\, \frac{\partial R(n,p)}{\partial n}\, h_n\, dx\, dt + \\ &+ \int_0^T \left(\int_{\Gamma_1} J\, \nu\, ds - f(t)\right)\left(\int_{\Gamma_1} (\mu_n \nabla h_n - \mu_n h_n \nabla V)\ \nu\, ds\right)\, dt\end{aligned} \tag{4.33}$$

with

$$\frac{\partial R(n,p)}{\partial n}\, h_n = \frac{p\,(\tau_p\,(n+\sigma^2) + \tau_n\,(p+\sigma^2)) - \tau_p\,(np - \sigma^4)}{(\tau_p\,(n+\sigma^2) + \tau_n\,(p+\sigma^2))^2}\, h_n$$

With the same approach the other partial derivatives are obtained as

$$\begin{aligned}\frac{\partial \mathcal{L}}{\partial p}\, h_p = &\int_0^T\!\!\int_\Omega (\lambda_1 - \frac{\partial \lambda_3}{\partial t})\, h_p\, dx\, dt + \int_\Omega \lambda_3(x,T)\, h_p(x,T)\, dx - \\ &- \int_0^T\!\!\int_\Omega \mu_p \Delta\lambda_3\, h_p\, dx\, dt + \int_0^T\!\!\int_{\partial\Omega} \mu_p\, \nabla\lambda_3\, h_p\, \nu\, ds\, dt + \\ &+ \int_0^T\!\!\int_\Omega \mu_p \nabla\lambda_3 \nabla V h_p\, dx\, dt - \int_0^T\!\!\int_{\partial\Omega} \mu_p\, \lambda_3(\nabla h_p + h_p \nabla V)\, \nu\, ds\, dt + \\ &+ \int_0^T\!\!\int_\Omega (\lambda_2 + \lambda_3)\, \frac{\partial R(n,p)}{\partial p}\, h_p\, dx\, dt + \\ &+ \int_0^T \left(\int_{\Gamma_1} J\, \nu\, ds - f(t)\right)\left(\int_{\partial\Omega} -\mu_p\,(\nabla h_p + h_p \nabla V)\, \nu\, ds\right)\, dt\end{aligned} \tag{4.34}$$

with

$$\frac{\partial R(n,p)}{\partial p}\, h_p = \frac{n\,(\tau_p\,(n+\sigma^2) + \tau_n\,(p+\sigma^2)) - \tau_n\,(np - \sigma^4)}{(\tau_p\,(n+\sigma^2) + \tau_n\,(p+\sigma^2))^2}\, h_p$$

$$\begin{aligned}\frac{\partial \mathcal{L}}{\partial V}\, h_V = &\int_0^T\!\!\int_\Omega \lambda^2\, \Delta\lambda_1\, h_V\, dx\, dt + \int_0^T\!\!\int_{\partial\Omega} \lambda^2\, \lambda_1\, \nabla h_V\, \nu\, ds\, dt - \\ &- \int_0^T\!\!\int_{\partial\Omega} \lambda^2\, \nabla\lambda_1\, h_V\, \nu\, ds\, dt + \int_0^T\!\!\int_\Omega \mu_n\, n\, \Delta\lambda_2\, h_V\, dx\, dt - \\ &- \int_0^T\!\!\int_{\partial\Omega} \mu_n\, \nabla\lambda_2\, n\, h_V\, \nu\, ds\, dt + \int_0^T\!\!\int_{\partial\Omega} \mu_n\, \lambda_2\, n\, \nabla h_V\, \nu\, ds\, dt - \\ &- \int_0^T\!\!\int_\Omega \mu_p\, p\, \Delta\lambda_3\, h_V\, dx\, dt + \int_0^T\!\!\int_{\partial\Omega} \mu_p\, \nabla\lambda_3\, p\, h_V\, \nu\, ds\, dt - \\ &- \int_0^T\!\!\int_{\partial\Omega} \mu_p\, p\, \lambda_3\, \nabla h_V\, \nu\, ds\, dt + \\ &+ \int_0^T \left(\int_{\Gamma_1} J\, \nu\, ds - f(t)\right)\left(\int_{\partial\Omega} (-\mu_n\, n\nabla h_V + \mu_p\, p\nabla h_V)\ \nu\, ds\right) dt\end{aligned} \tag{4.35}$$

$$\begin{aligned}\frac{\partial \mathcal{L}}{\partial V_0}\, h_{V_0} = &\int_\Omega -\lambda_2(x,0)\, \sigma^2\, e^{V_0}\, h_{V_0} dx + \int_\Omega \lambda_3(x,0)\, \sigma^2 e^{-V_0}\, h_{V_0}\, dx + \\ &+ \int_\Omega \lambda^2 \Delta\lambda_4\, h_{V_0}\, dx - \int_{\partial\Omega} \lambda^2\, \nabla\lambda_4\, h_{V_0}\, \nu\, ds + \int_{\partial\Omega} \lambda^2\, \lambda_4\, \nabla h_{V_0}\, \nu\, ds - \\ &- \int_\Omega \lambda_4\, \sigma^2\, e^{V_0}\, h_{V_0}\, dx - \int \lambda_4\, \sigma^2 e^{-V_0}\, h_{V_0}\, dx\end{aligned} \tag{4.36}$$

Depending on the choice of regularization the derivative of the Lagrange functional $\mathcal{L}$ with respect to the doping profile C is given by

$$\frac{\partial \mathcal{L}}{\partial C}\, h_C = \int_0^T\!\!\int_\Omega \lambda_1\, h_C\, dx\, dt + \int_\Omega \lambda_4\, h_C\, dx + \alpha \int_\Omega (C - C^*)\nabla C\, h_C\, dx \tag{4.37}$$

for Tikhonov regularization and like

$$\frac{\partial \mathcal{L}}{\partial C}\, h_C = \int_0^T\!\!\int_\Omega \lambda_1\, h_C\, dx\, dt + \int_\Omega \lambda_4\, h_C\, dx + \alpha \int_\Omega \frac{\nabla C}{\sqrt{|\nabla C|^2 + \beta}}\, \nabla h_C\, dx \tag{4.38}$$

for total variation regularization with $\beta > 0$.
Since the variations h are arbitrary, we obtain the equivalent system in $\Omega \times [0,T]$

$$-\lambda_1 - \frac{\partial \lambda_2}{\partial t} - \mu_n \, \Delta\lambda_2 - \mu_n \, \nabla V \, \nabla\lambda_2 + (\lambda_2 + \lambda_3)\frac{\partial R}{\partial n} = 0 \tag{4.39a}$$

$$\lambda_1 - \frac{\partial \lambda_3}{\partial t} - \mu_p \, \Delta\lambda_3 + \mu_p \, \nabla V \, \nabla\lambda_3 + (\lambda_2 + \lambda_3)\frac{\partial R}{\partial p} = 0 \tag{4.39b}$$

$$\lambda^2 \Delta\lambda_1 + \mu_n \, n \, \Delta\lambda_2 - \mu_p \, p \, \Delta\lambda_3 = 0 \tag{4.39c}$$

and in Ω

$$\lambda^2 \, \Delta\lambda_4 - \sigma^2 \, \lambda_4 \, (e^{V_0} + e^{-V_0}) = RS \tag{4.39d}$$

where the right hand side is given by

$$RS = \sigma^2 \, (\lambda_2(\cdot, 0) \, e^{V_0} - \lambda_3(\cdot, 0) \, e^{-V_0}).$$

The Dirichlet boundary conditions are

$$\lambda_2 = \int_{\partial\Omega} [\mu_n(\nabla n - n\nabla V) - \mu_p(\nabla p + p \, \nabla V)] \, \nu \, ds - f(t) \qquad \text{on } \Gamma_1 \times [0,T] \tag{4.40a}$$

$$\lambda_3 = -\int_{\partial\Omega} [\mu_n(\nabla n - n\nabla V) - \mu_p(\nabla p + p \, \nabla V)] \, \nu \, ds + f(t) \quad \text{on } \Gamma_1 \times [0,T] \tag{4.40b}$$

$$\lambda_2 = 0 \qquad \text{on } \Gamma_2 \times [0,T] \tag{4.40c}$$

$$\lambda_3 = 0 \qquad \text{on } \Gamma_2 \times [0,T] \tag{4.40d}$$

$$\lambda_1 = 0 \qquad \text{on } \partial\Omega_D \times [0,T] \tag{4.40e}$$

$$\lambda_4 = 0 \qquad \text{on } \partial\Omega_D \tag{4.40f}$$

and homogeneous Neumann boundary conditions. The terminal conditions are given by:

$$\lambda_2(x,T) = \lambda_3(x,T) = 0 \qquad \forall x \in \Omega \tag{4.41}$$

For a one dimensional semiconductor device on the scaled domain $\Omega = [0,1]$ we obtain the following adjoint equations

$$-\lambda_1 - \frac{\partial \lambda_2}{\partial t} - \mu_n \frac{\partial^2 \lambda_2}{\partial x^2} - \mu_n \frac{\partial V}{\partial x}\frac{\partial \lambda_2}{\partial x} + (\lambda_2 + \lambda_3)\frac{\partial R}{\partial n} = 0 \tag{4.42a}$$

$$\lambda_1 - \frac{\partial \lambda_3}{\partial t} - \mu_p \frac{\partial^2 \lambda_3}{\partial x^2} + \mu_p \frac{\partial V}{\partial x}\frac{\partial \lambda_3}{\partial x} + (\lambda_2 + \lambda_3)\frac{\partial R}{\partial p} = 0 \tag{4.42b}$$

$$\lambda^2 \frac{\partial^2 \lambda_1}{\partial x^2} + \mu_n\, n \frac{\partial^2 \lambda_2}{\partial x^2} - \mu_p\, p \frac{\partial^2 \lambda_3}{\partial x^2} = 0 \tag{4.42c}$$

with the boundary conditions

$$\lambda_2(1,t) = [\mu_n(\frac{\partial n}{\partial x} - n\frac{\partial V}{\partial x}) - \mu_p(\frac{\partial p}{\partial x} + p\frac{\partial V}{\partial x})] \mid_{x=1} - f(t) \tag{4.43a}$$

$$\lambda_3(1,t) = -[\mu_n(\frac{\partial n}{\partial x} - n\frac{\partial V}{\partial x}) - \mu_p(\frac{\partial p}{\partial x} + p\frac{\partial V}{\partial x})] \mid_{x=1} + f(t) \tag{4.43b}$$

$$\lambda_2(0,t) = 0 \quad \lambda_3(0,t) = 0 \tag{4.43c}$$

$$\lambda_1(1,t) = \lambda_1(0,t) = 0 \tag{4.43d}$$

$$\lambda_4(1) = \lambda_4(0) = 0 \tag{4.43e}$$

for $t \in [0,T]$, and the terminal conditions

$$\lambda_2(x,T) = \lambda_3(x,T) = 0$$

for $x \in (0,1)$.

Capacitance Measurements

In order to compute the capacitance of a semiconductor device one has to solve the linearized drift-diffusion equations with respect to applied voltage ϕ, in our case around $U \equiv 0$, which are given by (3.24). Therefore one has to solve the DD-model in thermal equilibrium first. The constraints of (4.17) or (4.20) are the linearized DDE and the DDE in thermal equilibrium. The corresponding

Lagrange functional is given by:

$$\begin{aligned}\mathcal{L}(\hat{n},\hat{p},\hat{V},V_0,\lambda_1,\lambda_2,\lambda_3,\lambda_4) = &\int_0^T\!\!\int_\Omega \lambda_1\ (\lambda^2\ \Delta\hat{V} - \hat{n} + \hat{p})\ dx\ dt + \\ &+ \int_0^T\!\!\int_\Omega \lambda_2\ \left(\frac{\partial \hat{n}}{\partial t} - \operatorname{div}\left(\mu_n\ \left(\nabla\hat{n} - \hat{n}\ \nabla V_0 - \sigma^2\ e^{V_0}\nabla\hat{V}\right)\right)\right)\ dx\ dt + \\ &+ \int_0^T\!\!\int_\Omega \lambda_3\ \left(\frac{\partial \hat{p}}{\partial t} - \operatorname{div}\left(\mu_p\ \left(\nabla\hat{p} + \hat{p}\ \nabla V_0 + \sigma^2\ e^{-V_0}\nabla\hat{V}\right)\right)\right)\ dx\ dt + \\ &+ \int_\Omega \lambda_4\ \left(\lambda^2\ \Delta V_0 - \sigma^2\ e^{V_0} + \sigma^2\ e^{-V_0} + C\right)\ dx + \\ &+ \int_0^T \left|\int_{\Gamma_1} \frac{\partial \hat{V}}{\partial \nu}\ ds - q(t)\right|^2 dt + \alpha \int_\Omega |C - C^*|^2\, dx\end{aligned} \tag{4.44}$$

Integration by parts with respect to the time yields

$$\begin{aligned}\mathcal{L} = &\int_0^T\!\!\int_\Omega \lambda_1\ (\lambda^2\ \Delta\hat{V} - \hat{n} + \hat{p})\ dx\ dt - \\ &- \int_0^T\!\!\int_\Omega \frac{\partial \lambda_2}{\partial t}\ \hat{n}\ dx\ dt + \int_\Omega \lambda_2(x,T)\ \hat{n}(x,T)\ dx - \\ &- \int_\Omega \lambda_2(x,0)\ \overbrace{\hat{n}(x,0)}^{=\sigma^2 e^{V_0}\hat{V}(x,0)}\ dx - \\ &- \int_0^T\!\!\int_\Omega \lambda_2\ \left(\operatorname{div}\left(\mu_n\ \left(\nabla\hat{n} - \hat{n}\ \nabla V_0 - \sigma^2\ e^{V_0}\nabla\hat{V}\right)\right)\right)\ dx\ dt + \\ &- \int_0^T\!\!\int_\Omega \frac{\partial \lambda_3}{\partial t}\ \hat{p}\ dx\ dt + \int_\Omega \lambda_3(x,T)\ \hat{p}(x,T)\ dx - \\ &- \int_\Omega \lambda_3(x,0)\ \overbrace{\hat{p}(x,0)}^{=\sigma^2\ e^{-V_0}\hat{V}(x,0)}\ dx - \\ &- \int_0^T\!\!\int_\Omega \lambda_3\ \left(\operatorname{div}\left(\mu_p\ \left(\nabla\hat{p} + \hat{p}\ \nabla V_0 + \sigma^2\ e^{-V_0}\nabla\hat{V}\right)\right)\right)\ dx\ dt + \\ &+ \int_\Omega \lambda_4\ \left(\lambda^2 \Delta V_0 - \sigma^2\ e^{V_0} + \sigma^2\ e^{-V_0} + C\right)\ dx + \\ &+ \int_0^T \left|\int_{\Gamma_1} \frac{\partial \hat{V}}{\partial \nu}\ ds - q(t)\right|^2 dt + \alpha \int_\Omega |C - C^*|^2\, dx\end{aligned} \tag{4.45}$$

The partial derivative with respect to $\hat{n}$ in direction $h_{\hat{n}}$ is

$$\begin{aligned}\frac{\partial \mathcal{L}}{\partial \hat{n}}\, h_{\hat{n}} = &\int_0^T\!\!\int_\Omega \left(-\lambda_1 - \frac{\partial \lambda_2}{\partial t}\right)\, h_{\hat{n}}\, dx\, dt + \int_\Omega \lambda_2(x,T)\, h_{\hat{n}}(x,T)\, dx - \\ &- \int_0^T\!\!\int_\Omega \mu_n\, \Delta\lambda_2\, h_{\hat{n}}\, dx\, dt + \int_0^T\!\!\int_{\partial\Omega} \mu_n\, \nabla\lambda_2\, h_{\hat{n}}\, \nu\, ds\, dt - \\ &- \int_0^T\!\!\int_\Omega \mu_n\, \nabla\lambda_2 \nabla V_0\, h_{\hat{n}}\, dx\, dt - \int_0^T\!\!\int_{\partial\Omega} \mu_n\, \lambda_2\, (\nabla h_{\hat{n}} - h_{\hat{n}} \nabla V_0)\, \nu\, ds\, dt\end{aligned} \tag{4.46}$$

The partial derivative with respect to $\hat{p}$ in direction $h_{\hat{p}}$ is

$$\begin{aligned}\frac{\partial \mathcal{L}}{\partial \hat{p}}\, h_{\hat{p}} = &\int_0^T\!\!\int_\Omega \left(\lambda_1 - \frac{\partial \lambda_3}{\partial t}\right)\, h_{\hat{p}}\, dx\, dt + \int_\Omega \lambda_3(x,T)\, h_{\hat{p}}(x,T)\, dx - \\ &- \int_0^T\!\!\int_\Omega \mu_p\, \Delta\lambda_3\, h_{\hat{p}}\, dx\, dt + \int_0^T\!\!\int_{\partial\Omega} \mu_p\, \nabla\lambda_3\, h_{\hat{p}}\, \nu\, ds\, dt + \\ &+ \int_0^T\!\!\int_\Omega \mu_p \nabla\lambda_3 \nabla V_0\, h_{\hat{p}}\, dx\, dt - \int_0^T\!\!\int_{\partial\Omega} \mu_p\, \lambda_3\, (\nabla h_{\hat{p}} + h_{\hat{p}} \nabla V_0)\, \nu\, ds\, dt\end{aligned} \tag{4.47}$$

The partial derivative with respect to $\hat{V}$ in direction $h_{\hat{V}}$ is

$$\begin{aligned}\frac{\partial \mathcal{L}}{\partial \hat{V}}\, h_{\hat{V}} = &\int_0^T\!\!\int_\Omega \lambda^2\, \Delta\lambda_1\, h_{\hat{V}}\, dx\, dt - \int_0^T\!\!\int_{\partial\Omega} \lambda^2\, \nabla\lambda_1\, h_{\hat{V}}\, \nu\, ds\, dt + \\ &+ \int_0^T\!\!\int_{\partial\Omega} \lambda^2 \lambda_1 \nabla h_{\hat{V}}\, \nu\, ds\, dt + \int_0^T\!\!\int_\Omega \mu_n\, \Delta\lambda_2\, \sigma^2\, e^{V_0}\, h_{\hat{V}}\, dx\, dt - \\ &- \int_0^T\!\!\int_{\partial\Omega} \mu_n \nabla\lambda_2\, \sigma^2\, e^{V_0}\, h_{\hat{V}}\, ds\, dt + \int_0^T\!\!\int_{\partial\Omega} \mu_n\, \lambda_2\, \sigma^2\, e^{V_0} \nabla h_{\hat{V}}\, \nu\, ds\, dt - \\ &- \int_0^T\!\!\int_\Omega \mu_p\, \Delta\lambda_3\, \sigma^2\, e^{-V_0}\, h_{\hat{V}}\, dx\, dt + \\ &+ \int_0^T\!\!\int_{\partial\Omega} \mu_n \nabla\lambda_3\, \sigma^2\, e^{-V_0}\, h_{\hat{V}}\, \nu\, ds\, dt - \\ &- \int_0^T\!\!\int_{\partial\Omega} \mu_p\, \lambda_3\, \sigma^2\, e^{-V_0}\, \nabla h_{\hat{V}}\, \nu\, ds\, dt + \int_\Omega \left(\int_{\Gamma_1} \frac{\partial \hat{V}}{\partial \nu}\, ds - q(t)\right) \nabla h_{\hat{V}}\, dt\end{aligned} \tag{4.48}$$

The partial derivative with respect to V_0 in direction h_{V_0} is

$$\begin{aligned}\frac{\partial \mathcal{L}}{\partial V_0}\, h_{V_0} = &\int_0^T\!\!\int_\Omega \mu_n\, \Delta\lambda_2\, \hat{n}\, h_{V_0}\, dx\, dt - \int_0^T\!\!\int_\Omega \nabla\lambda_2\, \sigma^2 e^{V_0}\, \nabla\hat{V}\, h_{V_0}\, dx\, dt - \\ &- \int_\Omega \lambda_2(x,0)\, \sigma^2\, e^{V_0}\, \hat{V}(x,0)\, h_{V_0}\, dx - \int_0^T\!\!\int_\Omega \mu_p\, \Delta\lambda_3\, \hat{p}\, h_{V_0}\, dx\, dt - \\ &- \int_0^T\!\!\int_\Omega \nabla\lambda_3\, \sigma^2\, e^{-V_0}\, \nabla\hat{V}\, h_{V_0}\, dx\, dt + \\ &+ \int_\Omega \lambda_3(x,0)\, \sigma^2\, e^{-V_0}\, h_{V_0}(x,0)\, dx + \\ &+ \int_\Omega \lambda^2 \Delta\lambda_4\, h_{V_0}\, dx - \int_\Omega \lambda_4\, \sigma^2 e^{V_0}\, h_{V_0}\, dx - \int_\Omega \lambda_4\, \sigma^2\, e^{-V_0}\, h_{V_0}\, dx\end{aligned} \tag{4.49}$$

Again, the partial derivative with respect to C is depending on the choice of regularization functional , we have

$$\frac{\partial \mathcal{L}}{\partial C}\, h_C = \int_\Omega \lambda_4\, h_C\, dx + \alpha \int_\Omega (C - C^*) \nabla C\, h_C\, dx \tag{4.50}$$

for Tikhonov regularization or

$$\frac{\partial \mathcal{L}}{\partial C}\, h_C = \int_\Omega \lambda_4\, h_C\, dx + \alpha \int_\Omega \frac{\nabla C}{\sqrt{|\nabla C|^2 + \beta}}\, \nabla h_C\, dx \tag{4.51}$$

for total variation regularization with $\beta > 0$.
Since the variations h are arbitrary, we obtain the equivalent system in $\Omega \times [0, T]$

$$\lambda^2\, \Delta\lambda_1 + \mu_n\, \sigma^2\, e^{V_0}\, \Delta\lambda_2 - \mu_p\, \sigma^2\, e^{-V_0}\, \Delta\lambda_2 = 0 \tag{4.52a}$$

$$-\lambda_1 - \frac{\partial \lambda_2}{\partial t} - \mu_n\, \Delta\lambda_2 - \mu_n\, \nabla V_0\, \nabla\lambda_2 = 0 \tag{4.52b}$$

$$\lambda_1 - \frac{\partial \lambda_3}{\partial t} - \mu_p\, \Delta\lambda_3 + \mu_p\, \nabla V_0\, \nabla\lambda_3 = 0 \tag{4.52c}$$

and in Ω

$$\lambda^2 \Delta\lambda_4 - \sigma^2\, e^{V_0} \lambda_4 - \sigma^2\, e^{-V_0} \lambda_4 = RS \tag{4.52d}$$

where the right hand side is given by

$$\begin{aligned} RS = &\int_0^T \left(-\mu_n\, \hat{n}\, \Delta\lambda_2 + \sigma^2\, e^{V_0}\, \nabla\hat{V}\, \nabla\lambda_2\right) dt + \\ &+ \int_0^T \left(\mu_p\, \hat{p}\, \Delta\lambda_3 + \sigma^2\, e^{-V_0}\, \nabla\hat{V}\, \nabla\lambda_3\right) dt + \\ &+ \lambda_2(x,0)\, \sigma^2\, e^{V_0}\, \hat{V}(x,0) - \lambda_3(x,0)\, \sigma^2\, e^{-V_0}\, \hat{V}(x,0) \end{aligned} \tag{4.53}$$

The corresponding Dirichlet boundary conditions on $\partial\Omega_D = \Gamma_1 \cup \Gamma_2$, $\Gamma_1 \cap \Gamma_2 = \emptyset$ are

$$\lambda_1 = -\frac{1}{\lambda^2}\left(\frac{\partial\hat{V}}{\partial\nu} - q(t)\right) \quad \text{on } \Gamma_1 \times [0,T] \tag{4.54a}$$

$$\lambda_1 = 0 \quad \text{on } \Gamma_2 \times [0,T] \tag{4.54b}$$

$$\lambda_2 = 0 \quad \text{on } \partial\Omega_D \times [0,T] \tag{4.54c}$$

$$\lambda_3 = 0 \quad \text{on } \partial\Omega_D \times [0,T] \tag{4.54d}$$

$$\lambda_4 = 0 \quad \text{on } \partial\Omega_D \tag{4.54e}$$

and homogeneous Neumann boundary conditions. Instead of initial conditions the following end conditions hold:

$$\lambda_2(x,T) = 0 \quad \lambda_3(x,T) = 0 \quad \forall x \in \Omega \tag{4.55}$$

Remark

Independent of the choice of measurements either capacitance or current measurements one has to solve a system of partial differential equations backwards in time.

This can be illustrated by considering a simple model problem, namely the parabolic partial differential equation

$$\frac{\partial u}{\partial t} = \Delta u$$

on a bounded area Ω with initial conditions

$$u(x,0) = \phi(x)$$

and boundary conditions

$$u = f \quad \text{on } \partial\Omega_D \times [0,T]$$
$$\frac{\partial u}{\partial n} = g \quad \text{on } \partial\Omega_N \times [0,T]$$

Solving the equation forward in time damps high oscillations, while solving it backward amplifies errors. Considering the adjoint problems (4.39) and (4.52) these problems do not occur. The model analogue of both cases look like

$$\frac{\partial u}{\partial t} = -\Delta u$$

Due to the sign change a reversed behavior can be observed - solving the equation backward in time does not cause any instabilities, while solving it forward would be ill-posed.

Algorithm

From the analysis of the preceding sections we can derive the following algorithm for the minimization problem (4.17).
Input: initial value $C^* = C^*(x)$, applied potential $U = U(x,t)$, measured flow $f = f(t)$ or measured capacitance $q = q(t)$

(1) Solve DD-model in thermal equilibrium to obtain V_0

   (a) Solve the drift diffusion equations (3.18) for C_k to obtain (V, n, p) and the total current flow J given by (4.1)

   (b) Solve the linearized drift - diffusion equations (4.9) to obtain $(\hat{V}, \hat{n}, \hat{p})$ and the capacitance Cap given by (4.2).

(2) Solve (4.39) and or (4.52) for $(\lambda_1, \lambda_2, \lambda_3, \lambda_4)$

(3) Calculate $\frac{\partial \mathcal{L}}{\partial C}(C_k) = \frac{dQ}{dC}(C_k)$

(4) Determine C_{k+1} using gradient based methods such as steepest descent

(5) If convergence criterion is satisfied stop, else return to (1)

Both (3.18) and (4.9) are systems of time dependent partial differential equations, the computation of the solutions is quite time consuming. For the reconstruction of the doping profile one can use either current measurements and/or capacitance measurements. Using both types of measurements require the solution of five systems of partial differential equations, first the equilibrium solution, then the drift - diffusion equations and their linearization and finally their sensitivities. This causes a very high numerical effort in the reconstruction algorithm even in the one dimensional case.

Chapter 5

Uniqueness and Non-uniqueness

For the drift-diffusion equations a lot of analytical work has been done in the last decades (c.f. [11],[18],[17],[16]). For both the steady state and the transient case, the existence of a solution has been shown. Considering uniqueness the transient case is easier to deal with, since it has globally unique solutions even for large voltages, which is not the case in the steady state DD-model. Gajewski proved in [11] that for the transient drift-diffusion equations a unique solution exists. In the steady state case uniqueness results were presented under the assumption that the applied voltage is small (c.f.[4]).

The main focus in this section is the question whether the data determines the doping profile uniquely. In mathematical terms this question is called the identifiability, which determines whether the parameter-to-output map F is injective.

In numerical experiments severe difficulties appeared reconstructing the doping profile in case of a np-diode. In [4] it is shown that in spatial dimensional one the doping profile of a unipolar diode can be identified uniquely from a single transient measurement. Still additional smoothness assumptions are required. The doping profile is assumed to be a continuously differentiable function whose partial derivatives are Hölder continuous derivative with exponent $\alpha = 1$, i.e. $C \in C^{1,1}(\Omega)$. In case of discontinuous doping profiles these results do not hold. So far there has been no results on the unipolar multi-dimensional inverse doping problem. For more general devices like np-diodes no uniqueness results have been

derived yet.
In the following some analytical and numerical results are presented, which show the existence of multiple solutions in the bipolar case, concerning a simplified model.
Throughout this section only the one dimensional case is considered and the following assumptions are made:

- The mobilities of the electrons and holes are equal, i.e. $\mu_n = \mu_p$
- The relaxation times of the electrons and holes are equal, i.e. $\tau_n = \tau_p$

Under these assumptions we can show that the inverse problem for the drift-diffusion equations, considering both current and capacitance measurements admits at least two solutions.

Proposition 5.1. There exist at least two solutions $C_i \in H^1(\Omega)$, $i = 1, 2$ to the inverse problem for the drift-diffusion equations (3.13). In particular, if (n_1, p_1, V_1, C_1) is a solution of (3.13) there exists a second solution (n_2, p_2, V_2, C_2) given by

$$C_2(x) = -C_1(1-x), \tag{5.1a}$$
$$n_2(x,t) = p_1(1-x,t), \tag{5.1b}$$
$$p_2(x,t) = n_1(1-x,t), \tag{5.1c}$$
$$V_2(x,t) = -V_1(1-x,t) + U(x,t), \tag{5.1d}$$

such that

$$J_{n_2} = J_{p_1}, \quad J_{p_2} = J_{n_1}$$
$$Cap\,(V_2) = Cap\,(V_1)$$

Proof. Defining a new variable $\xi = 1 - x$ the following calculations can be done

$$\begin{aligned}
J_{n_2}(x,t) &= \frac{\partial n_2}{\partial x}(x,t) - n_2(x,t)\,\frac{\partial V_2}{\partial x}(x,t) \\
&= -\frac{\partial p_1}{\partial \xi}(\xi,t) - p_1(\xi,t)\,\frac{\partial V_1}{\partial \xi}(\xi,t) = J_{p_1}(\xi,t) \\
J_{p_2}(x,t) &= -\frac{\partial p_2}{\partial x}(x,t) - p_2(x,t)\,\frac{\partial V_2}{\partial x}(x,t) \\
&= \frac{\partial n_1}{\partial \xi}(\xi,t) - n_1(\xi,t)\,\frac{\partial V_1}{\partial \xi}(\xi,t) = J_{n_1}(\xi,t) \\
R(x,t) &= \frac{n_2(x,t)\,p_2(x,t) - \sigma^4}{\tau\,(p_2(x,t)+\sigma^2) + \tau\,(n_2(x,t)+\sigma^2)} \\
&= \frac{p_1(\xi,t)\,n_1(\xi,t) - \sigma^4}{\tau\,(n_1(\xi,t)+\sigma^2) + \tau\,(p_1(\xi,t)+\sigma^2)} = R(\xi,t)
\end{aligned}$$

It can be calculated in a straight forward way

$$\begin{aligned}
\frac{\partial n_2}{\partial t}(x,t) = \frac{\partial p_1}{\partial t}(\xi,t) &= -\frac{\partial}{\partial \xi}\left(\mu\, J_{p_1}(\xi,t)\right) - R(\xi,t) \\
&= \frac{\partial}{\partial x}\left(\mu\, J_{n_2}(x,t)\right) - R(x,t) \\
\frac{\partial p_2}{\partial t}(x,t) = \frac{\partial n_1}{\partial t}(\xi,t) &= -\frac{\partial}{\partial \xi}\left((\mu\, J_{n_1}(\xi,t)\right) - R(\xi,t) \\
&= \frac{\partial}{\partial x}\left(\mu\, J_{p_2}(x,t)\right) - R(x,t)
\end{aligned}$$

Furthermore one obtains that

$$\begin{aligned}
\lambda^2\,\frac{\partial^2 V_2}{\partial x^2}(x,t) &= -\lambda^2\,\frac{\partial^2 V_1}{\partial \xi^2}(\xi,t) \\
&= -n_1(\xi,t) + p_1(\xi,t) + C_1(\xi,t) \\
&= -p_2(x,t) + n_1(x,t) - C_2(x,t)
\end{aligned}$$

We still have to show the equivalence of the capacitance measurements. In the one-dimensional setting the capacitance

$$\begin{aligned}
Cap\,(V_2) = \frac{\partial}{\partial U}\left(\frac{\partial V_2}{\partial x}(x,t)\right) &= \frac{\partial}{\partial U}\left(-\frac{\partial V_1}{\partial x}(1-x,t)\right) = \\
&= \frac{\partial}{\partial U}\left(\frac{\partial V_1}{\partial \xi}(\xi,t)\right) = Cap\,(V_1)
\end{aligned}$$

□

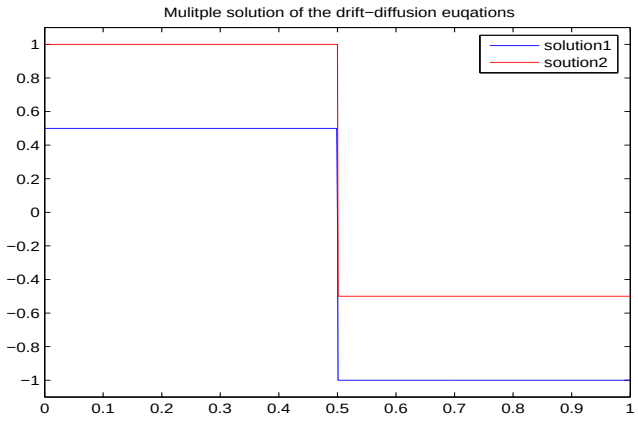

Figure 5.1: Multiple Solutions of the inverse dopant profiling

From the proof it can be seen that interchanging the roles of the electrons and holes allows the multiplicity of the solutions of the drift-diffusion equations. In Figure 5 two possible solutions of the inverse dopant problem are illustrated.

We consider Tikhonov regularization and obtain the minimization problem

$$Q_f(u,C) = |F(C) - f(t)|^2 + \alpha\,|C - C^*|^2 \to \min_C \tag{5.2}$$

where $f(t)$ denotes the current measurements or

$$Q_q(u,C) = |F(C) - q(t)|^2 + \alpha\,|C - C^*|^2 \to \min_C \tag{5.3}$$

where $q(t)$ refers to the capacitance measurements. The operator F maps either the doping profile C to the current or to the capacitance measured at a contact Γ_1. In both cases the weak sequential closedness of F, which has been shown in Section 4, ensures the existence of a solution for both minimization problems. Under the assumptions made above it has already been shown that the inverse problem admits multiple solutions, therefore one cannot expect unique minimizers of the Tikhonov functional.

Indeed it is possible to show that the multiple solutions are both minimizers of (5.2) and (5.3).

Proposition 5.2. The assumptions of Proposition 5.1 hold and

$$C^*(x) = -C^*(1-x).$$

Then there exist at least two minimizers of the optimization problem (5.2) and (5.3). The multiple solutions of the inverse problem given by (5.1) are minimizers of the Tikhonov functionals (5.2) and (5.3). Furthermore

$$Q_f(n_1, p_1, V_1, C_1) = Q_f(n_2, p_2, V_2, C_2)$$
$$Q_q(n_1, p_1, V_1, C_1) = Q_q(n_2, p_2, V_2, C_2)$$

holds.

Proof. It has already been shown that both minimizers are solutions of the drift - diffusion equations. Using the new variable $\xi = 1 - x$ one obtains

$$\begin{aligned}
Q_f(n_2, p_2, V_2, C_2) &= \int_0^T |J_{n_2}(x,t) + J_{p_2}(x,t) - f(t)|^2 \, dt + \\
&\quad + \alpha \int_0^1 |C_2(x,t) - C^*(x,t)|^2 \, dx \\
&= \int_0^T |J_{p_1}(\xi,t) + J_{n_1}(\xi,t) - f(t)|^2 \, dt + \\
&\quad + \alpha \int_0^1 |-C_1(\xi,t) + C^*(\xi,t)|^2 \, d\xi \\
&= \int_0^T |J_{p_1}(x,t) + J_{n_1}(x,t) - f(t)|^2 \, dt + \\
&\quad + \alpha \int_0^1 |C_1(x,t) - C^*(x,t)|^2 \, dx \\
&= Q_f(n_1, p_1, V_1, C_1)
\end{aligned}$$

In case of capacitance measurements we obtain

$$\begin{aligned}
Q_q(n_2,p_2,V_2,C_2) &= \int_0^T \left| \frac{\partial}{\partial U}\left(\frac{\partial V_2}{\partial x}(x,t)\right) - q(t)\right|^2 dt + \\
&\quad + \alpha \int_0^1 |C_2(x,t) - C^*(x,t)|^2\, dx = \\
&= \int_0^T \left| \frac{\partial}{\partial U}\left(\frac{\partial V_1}{\partial \xi}(\xi,t)\right) - q(t)\right|^2 dt + \\
&\quad + \alpha \int_0^1 |-C_1(\xi,t) + C^*(\xi,t)|^2\, dx = \\
&= \int_0^T \left| \frac{\partial}{\partial U}\left(\frac{\partial V_1}{\partial x}(x,t)\right) - q(t)\right|^2 dt + \\
&\quad + \alpha \int_0^1 |C_1(x,t) - C^*(x,t)|^2\, dx = \\
&= Q_q(n_1,p_1,V_1,C_1)
\end{aligned}$$

□

Using total variation regularization analogous results can be shown. We mention that our analysis of multiple solutions was motivated by similar results concerning the steady state DD-model (cf. [14]). Considering a slightly different minimization functional one could avoid the existence of the multiple solutions constructed above. This functional is given by:

$$\begin{aligned}
Q(u,C) = &\int_0^T \left| \int_{\Gamma_1} J_n\, d\nu - f_n(t)\right|^2 dt + \int_0^T \left| \int_{\Gamma_1} J_p\, d\nu - f_p(t)\right|^2 dt + \\
&+ \alpha \int_\Omega |\, C - C^*\,|^2\, dx
\end{aligned} \tag{5.4}$$

For (5.4) the couple (n_2,p_2,V_2,C_2) constructed as above is not a minimizer any more. This provides reasonable remedy for optimal design and optimal control tasks as considered in [14], but for the identification of the doping profile this means that one has to measure the current caused by the holes and the current caused by the electrons separately, which is not possible in practice !

Chapter 6

Piecewise Constant Doping Profiles

In Section 3.4 we presented a singular perturbation analysis for highly doped semiconductor devices. In order to employ this perturbation analysis one has to know the location of the pn-junction, which is usually not the case in practice. In this section we consider the reconstruction of piecewise constant doping profiles from current measurements in case of spatial dimension one. The doping profile C can be written as:

$$C = C_1\chi_n + C_2\chi_p \tag{6.1}$$

with given values $(C_1, C_2) =$ const and (χ_n, χ_p) are the indicator functions on the p or n regions.

The quantity to be identified is the location of the pn-junction γ, which separates the n-region and the p-region. In literature this problem is referred to as the inverse boundary problem - using given measurements on some Dirichlet boundary part one tries to compute the shape of an interior boundary γ.

Throughout the whole section we assume that the semiconductor device is in spatial dimension one and has a single junction $\gamma \in (0, 1)$. The abstract formulation of the inverse problem is given by:

$$F(\gamma) = Y^\delta \tag{6.2}$$

with

$$F\colon \mathbb{R} \to \mathbb{R} \tag{6.3}$$

$$\gamma \mapsto \Sigma_C \tag{6.4}$$

with Σ_C is given by

$$\begin{aligned}\Sigma_C : L^2([0,T], x_1) &\to L^2([0,T], x_2)\\ U &\mapsto J\mid_{x=x_2} = (J_n + J_p)\mid_{x=x_2}\end{aligned}$$

and $\Omega = [x_1, x_2]$.
One can show that the operator F is well-defined and Fréchet-differentiable:

Proposition 6.1. The map F is well-defined by (6.3), continuous and differentiable.

Proof. Using the same arguments as in Section 4 one can rewrite the operator F as follows:

$$\begin{aligned}F &= F_1 \circ F_2\\ F_2 &: \gamma \to (n, p, V)\\ F_1 &: (n, p, V) \to J \cdot \nu\end{aligned}$$

It can be shown that F_1 is well defined and Fréchet differentiable using the same arguments as in proof (4.1). The partial derivative of F_2 with respect to γ in the direction $(\hat{n}, \hat{p}, \hat{V})$ is given by:

$$\begin{aligned}\lambda^2 \frac{\partial^2 \hat{V}}{\partial x^2} &= \hat{n} - \hat{p} - [C]_{x=\gamma}\ \delta(\gamma)\\ \frac{\partial \hat{n}}{\partial t} &= \frac{\partial}{\partial x}(\mu_n(\frac{\partial \hat{n}}{\partial x} - \hat{n}\frac{\partial V}{\partial x} - n\frac{\partial \hat{V}}{\partial x}) - \hat{R}\\ \frac{\partial \hat{p}}{\partial t} &= \frac{\partial}{\partial x}(\mu_p(\frac{\partial \hat{p}}{\partial x} + \hat{p}\frac{\partial V}{\partial x} + p\frac{\partial \hat{V})}{\partial x} - \hat{R}\end{aligned}$$

where (V, n, p) denoted the solution of the drift-diffusion system (3.18). Integration of the Poisson equation

$$\lambda^2 \frac{\partial^2 V}{\partial x^2} = n - p - C$$

gives

$$V = \int_0^1 G(x,y)(n-p)\,dy - C_1 \int_0^\gamma G(x,y)\,dy - \\ - C_2 \int_0^\gamma G(x,y)\,dy - G(x,1)\,V(1) + G(x,0)\,V(0)$$

where G denotes the Green function of the Laplace operator given by

$$G(x,y) = 1 - |x-y|$$

V depends continuously on γ. With similar arguments as in the proof of Proposition 4.3 one can show that F_2 is well defined, continuous and Fréchet differentiable. □

Applying Tikhonov regularization to equation (6.2) one obtains

$$Q(u,\gamma) = \left(F(\gamma) - y^\delta\right)^2 + \alpha\,(\gamma - \gamma^*)^2 \to \min_{\gamma\in\mathbb{R}} \tag{6.5}$$

In spatial dimension one regularization is not really needed, because the problem is finite-dimensional. But including γ^* in the reconstruction gives an a-priori knowledge of the solution γ.

The partial derivative of the minimization functional (6.5) with respect to γ can be calculated using the adjoint or the direct approach - the computational effort is the same considering the one dimensional case. With the adjoint approach one can use the corresponding Lagrange functional to calculate the partial derivatives. As presented in Section 3.4 layer terms have to be defined when carrying out singular perturbation analysis.

We consider a unipolar device $\Omega = [0,1]$ with the junction at $x = \gamma$The corre-

sponding Lagrange functional $\mathcal{L}$ is

$$\begin{aligned}\mathcal{L} = &\int_0^{\lambda} \lambda_1 \,(\frac{\partial^2 V}{\partial x^2} - n + C)\, dx + \int_0^{\lambda} \lambda_2 \,[\frac{\partial}{\partial x}(\mu_n \,(\frac{\partial n}{\partial x} - n\frac{\partial V}{\partial x}))\, dx + \\ &+ \int_{\lambda}^{\gamma-\lambda} \lambda_1 \,(n - C)\, dx + \int_{\lambda}^{\gamma-\lambda} \lambda_2 \,(\mu_n \,(\frac{\partial n}{\partial x} - n\frac{\partial V}{\partial x}))\, dx + \\ &+ \int_{\gamma-\lambda}^{\gamma+\lambda} \lambda_1 \,(\frac{\partial^2 V}{\partial x^2} - n + C)\, dx + \int_{\gamma-\lambda}^{\gamma+\lambda} \lambda_2 \,[\frac{\partial}{\partial x}(\mu_n \,(\frac{\partial n}{\partial x} - n\frac{\partial V}{\partial x}))\, dx + \\ &+ \int_{\gamma+\lambda}^{1-\lambda} \lambda_1 \,(n - C)\, dx + \int_{\gamma+\lambda}^{1-\lambda} \lambda_2 \,(\mu_n \,(\frac{\partial n}{\partial x} - n\frac{\partial V}{\partial x}))\, dx + \\ &+ \int_{1-\lambda}^{1} \lambda_1 \,(\frac{\partial^2 V}{\partial x^2} - n + C)\, dx + \int_{1-\lambda}^{1} \lambda_2 \,[\frac{\partial}{\partial x}(\mu_n \,(\frac{\partial n}{\partial x} - n\frac{\partial V}{\partial x}))\, dx + \\ &+ \left|\mu_n \,(\frac{\partial n}{\partial x} - n\frac{\partial V}{\partial x}) - J\right|^2 + \alpha \,|\gamma - \gamma^*|^2\end{aligned} \tag{6.6}$$

Calculation of the partial derivatives with respect to (V, n) gives the following sensitivities within the layers $(x \in (0, \lambda) \cup (\gamma - \lambda, \gamma + \lambda) \cup (1 - \lambda, 1))$:

$$\frac{\partial^2 \lambda_1}{\partial x^2} + \mu_n \, n \, \frac{\partial^2 \lambda_2}{\partial x^2} = 0 \tag{6.7a}$$

$$-\lambda_1 - \mu_n \, \frac{\partial^2 \lambda_2}{\partial x^2} - \mu_n \, \frac{\partial V}{\partial x} \frac{\partial \lambda_2}{\partial x} = 0 \tag{6.7b}$$

In regions where the reduced equations $(x \in (\lambda, \gamma - \lambda) \cup (\gamma + \lambda, 1 - \lambda))$ hold one obtains:

$$\frac{\partial^2 \lambda_2}{\partial x^2} = 0 \tag{6.8a}$$

$$-\lambda_1 - \mu_n \, \frac{\partial^2 \lambda_2}{\partial x^2} - \mu_n \, \frac{\partial V}{\partial x} \frac{\partial \lambda_2}{\partial x} = 0 \tag{6.8b}$$

with continuous interface conditions. The Dirichlet boundary conditions are

$$\lambda_2(1) = \mu_n \,(\frac{\partial n}{\partial x} - n \, \frac{\partial V}{\partial x}) - f \tag{6.9}$$

$$\lambda_1(1) = \lambda_1(0) = \lambda_2(0) = 0 \tag{6.10}$$

The system can be simplified to

$$\lambda_2 = c_1 \, x + c_2$$

$$\lambda_1 = -\mu_n \, c_1 \, \frac{\partial V}{\partial x}$$

where c_1 and c_2 are constants such that continuous interface conditions are obtained. Only the doping profile C depends on γ, therefore the partial derivative of the Lagrange functional with respect to γ is given by:

$$\begin{aligned}\frac{\partial \mathcal{L}}{\partial \gamma} &= \frac{\partial}{\partial \gamma}\int_{\gamma-\lambda}^{\gamma} \lambda_1\, C\, dx + \frac{\partial}{\partial \gamma}\int_{\gamma-\lambda}^{\gamma} \lambda_1\, C\, dx + \alpha\,(\gamma-\gamma_0) = \\ &= \lambda_1(\gamma)_- C(\gamma)_- + \lambda_1(\gamma)_+ C(\gamma)_+ + \alpha\,(\gamma-\gamma_0) = \\ &= -\left[C\right]_{x=\gamma}\delta(\gamma)\;\lambda_1(\gamma) + \alpha\,(\gamma-\gamma_0)\end{aligned} \tag{6.11}$$

where $[C]_{x=\gamma}$ denotes the jump of the doping profile C at $x=\gamma$.
It is also possible to simultaneously reconstruct the parameters (C_1, C_2) in (6.1). Then the operator F would look like

$$F\colon \mathbb{R}^3 \to \mathbb{R} \tag{6.12}$$

$$(C_1, C_2, \gamma) \mapsto \Sigma_C \tag{6.13}$$

Using similar arguments one can show that the map F is well-defined, continuous and Fréchet-differentiable. The reconstruction of the junction is quite stable, while concerning (6.12) one needs to have good initial guess. The map (6.12) is underdetermined, therefore one has to apply regularization to obtain reasonable results. For the pn-diode an analogous treatment is possible in principle, but the numerical solution of the direct problem becomes quite involved and this issue is beyond the scope of this work.

6.1 Numerical Examples

In this section we present the reconstruction of the doping profile from a single current measurement.

The maximum doping concentration is $\tilde{C} = 10^{21}\ \mathrm{cm}^{-3}$ with the Debye length $\lambda = 1e^{-4}$. It has to be pointed out that $C(x) \neq 0$ in the reduced equations (3.28a), otherwise the system is under-determined.

The exact doping profile is given by

$$C(x) = \begin{cases} 1 & x \leq 0.5 \\ 0.1 & x > 0.5 \end{cases}$$

and the initial guess by

$$C_0(x) = \begin{cases} 1.01 & x \leq 0.6 \\ 0.11 & x > 0.6 \end{cases}$$

The reconstructed doping profile can be seen in Figure 6.1, the corresponding cost functional Q in 6.2.

It turns out that reconstruction of the pn-junction γ, with C_1 and C_2 known, is stable. We already mentioned that no regularization is needed to obtain reasonable results. If one wants to identify (C_1, C_2, γ) from a single measurement a good initial guess is needed to obtain a satisfactorily approximation. The loss of time dependency causes a significant decrease in numerical effort. After 22 iterations, which take about 15 minutes, the regularized solution is obtained.

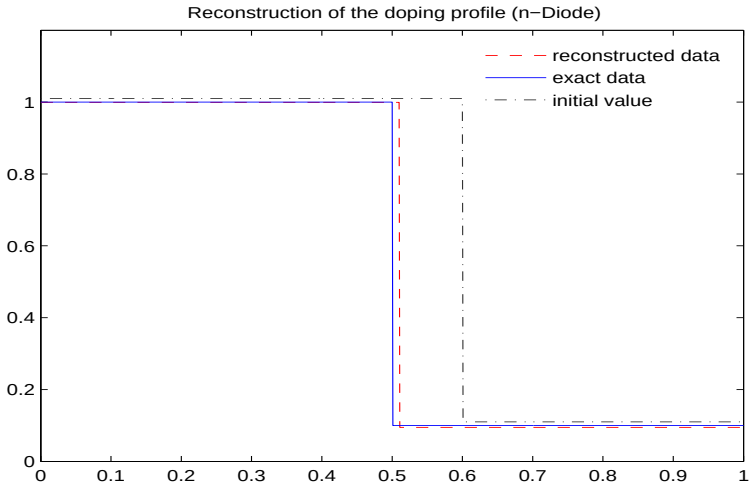

Figure 6.1: Reconstructed doping profile of a unipolar diode with asymptotic expansion

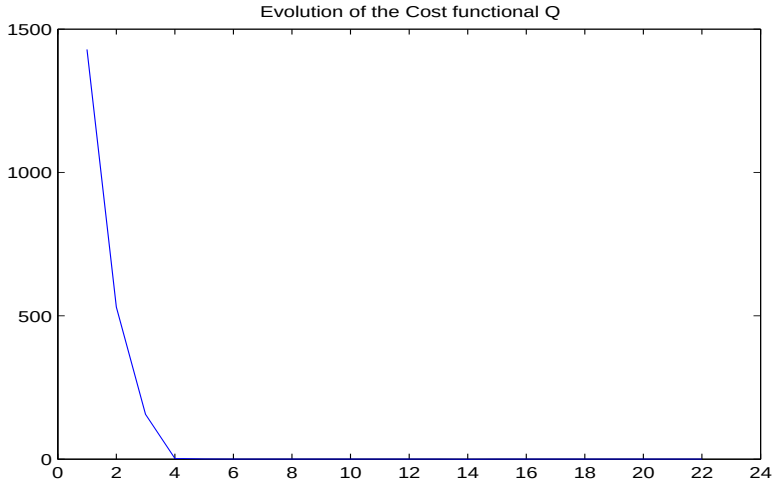

Figure 6.2: Evaluation of the cost functional

Chapter 7

Numerical Examples

In this section the results of numerical examples are presented. All computations have been performed on the software systems MATLOW 7 and FEMLAB 3.1. In our examples we used typical values of the parameters of silicon at room temperature $(T = 300K)$, which are listed in Table 7.1. To generate the problem data,

Parameter	Physical Meaning	Numerical Value
q	elementary charge	$1.6 \cdot 10^{-19}$ As
n_i	intrinsic density	10^{10} cm^{-3}
ϵ_S	permittivity constant	10^{-12} As V^{-1}s^{-1}
μ_n	mobility of electrons	$1.5 \cdot 10^3$ cm^{2}V^{-1}s^{-1}
μ_p	mobility of holes	10^3 cm^{2}V^{-1}s^{-1}
U_T	thermal voltage	0.0259 V
τ_n	lifetime of electrons	10^{-6} s
τ_p	lifetime of holes	10^{-5} s

Table 7.1: Physical parameters for silicon at room temperature

we solved the direct problem (3.18) and (3.24) for U. In order to avoid so called inverse crimes, these problems were solved on a very fine mesh using a piecewise linear finite element base. This mesh was different from the one we used to evaluate the gradient of the minimization functional (4.17) or (4.20).

7.1 n-Diode

The simplest semiconductor device is a one dimensional unipolar diode. The exact doping profile is given by

$$C(x) = \begin{cases} 1 & 0 \leq x \leq 0.5, \\ 0 & 0.5 < x \leq 1 \end{cases}$$

We choose a diode of length $L = 10^{-4}\,\mathrm{cm}$ and a maximum doping concentration of $\tilde{C} = 10^{16}\,\mathrm{cm}^{-3}$. The corresponding Debye length λ is approximately 0.04. The n-diode can be modeled using the unipolar scaled drift diffusion equations in the one-dimensional case, i.e.,

$$\lambda^2 \frac{\partial^2 V}{\partial x^2} = n - C \tag{7.1a}$$

$$\partial_t n = \frac{\partial}{\partial x}\left(\mu_n \left(\frac{\partial n}{\partial x} - n \frac{\partial V}{\partial x}\right)\right) \tag{7.1b}$$

For the applied time scaling we obtain

$$t = \frac{L^2}{U_T \tilde{\mu}} t_s = \frac{1e^{-8}}{1e^{-2}} t_s = 1e^{-6} s$$

when choosing $\tilde{\mu} = 1$.
In practice it seems reasonable to measure the current density every 10^{-4} seconds. In order to use these measurements one has to solve the drift -diffusion equations over a large time interval. For all numerical calculations the time increment was 10^2 running from 0 to 10^4. The applied voltage was

$$U(x,t) = 10^{-5}(t + \sin(t)).$$

Reconstructions have been performed using a projected steepest descent or a projected BFGS algorithm with the constraint that

$$C(x) \geq 0.$$

Reconstruction of the doping profile from current measurements:

Figure 7.1 shows the reconstructed doping profile of a unipolar diode using steepest descent algorithm and Tikhonov regularization. The evaluation of the corresponding cost function is given in Figure 7.2. After 30 iterations a regularized solution is obtained. The reconstructed solution is much smoother than the exact solution. The value of the cost functional Q is approximately 10^{-6}.

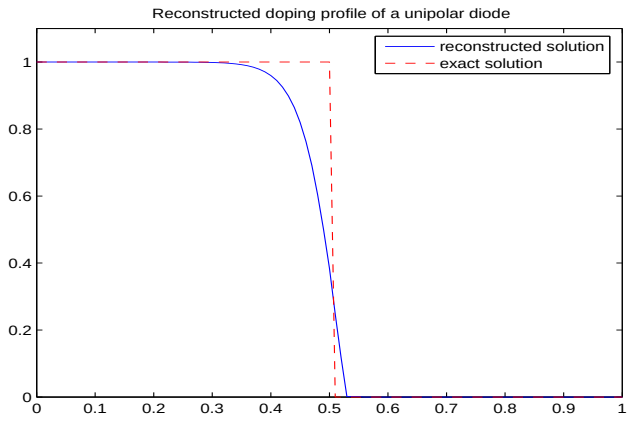

Figure 7.1: Reconstructed doping profile of a n-Diode using steepest descent

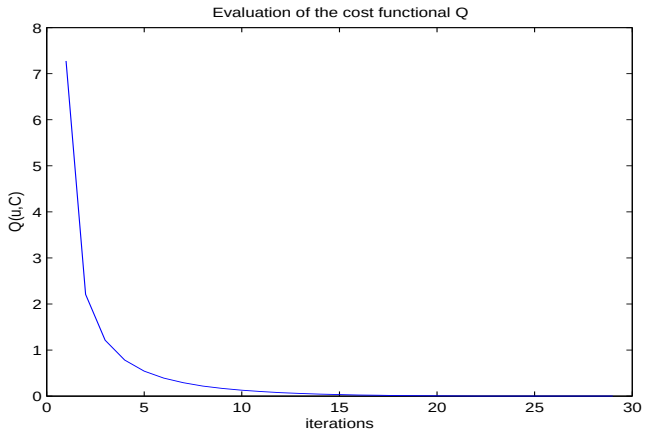

Figure 7.2: Evaluation of the cost functional Q

The reconstructed doping profile using BFGS iterations can be seen in Figure 7.3, the corresponding cost functional in Figure 7.4. Using the same initial guess the BFGS method is faster, only 19 iterations are needed. The reconstructed solution is very similar to the one obtained by Tikhonov regularization, the value of the cost functional Q is about 10^{-4}.

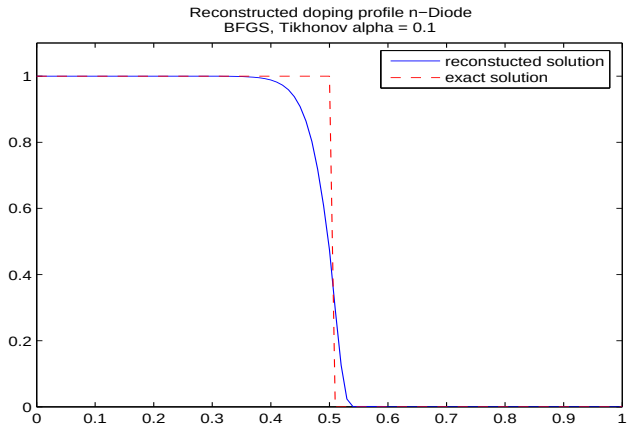

Figure 7.3: Reconstruction of the doping profile of a n-Diode using BFGS

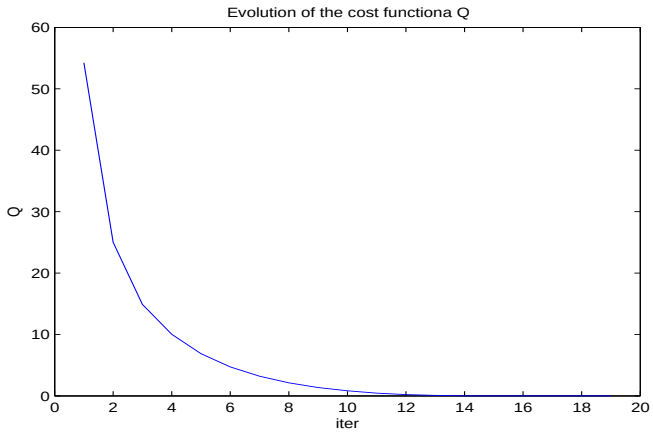

Figure 7.4: Evolution of the cost functional Q

We mentioned in Section 4.2 that total variation regularization favors sharp edges. In Figure 7.5 and 7.6 we see the regularized solution and the corresponding cost functional Q using total variation regularization. The solution is quite similar to the one obtained by Tikhonov regularization, but the gradient of the doping profile is steeper around the junction.

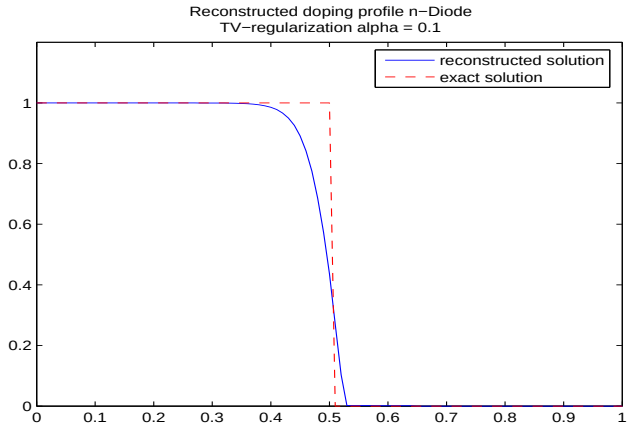

Figure 7.5: Reconstruction of the doping profile of a n-Diode using BFGS

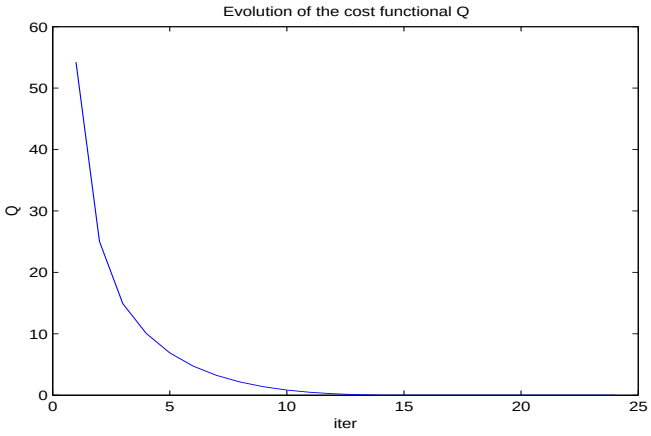

Figure 7.6: Evolution of the cost functional Q

In case of noise the choice of the regularization parameter is important for the quality of the regularized solution. According to the discrepancy principle 4.18 we choose the regularization parameter such that

$$\delta \leq \left| F(C) - Y^{\delta} \right| \leq \tau \, \delta \tag{7.2}$$

with $\tau = 1.1$. Figure 7.7 shows the regularized solution for $\delta = 5\%$.

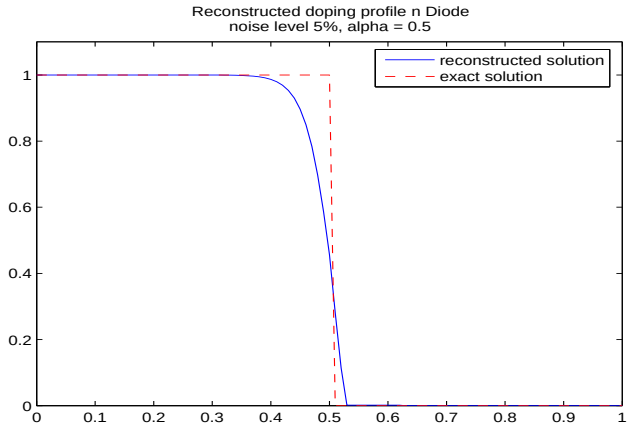

Figure 7.7: Reconstructed doping profile of a n-Diode $\delta = 5$

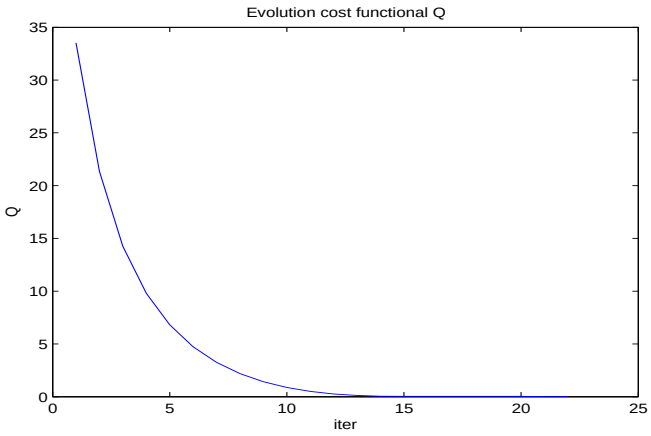

Figure 7.8: Evolution of the cost functional Q

Reconstruction of the doping profile from capacitance measurements:

The parameter values are the same as in the case of current measurements using Tikhonov regularization. The reconstructed doping profile and the corresponding cost functional can be seen in Figure 7.9 and 7.10.

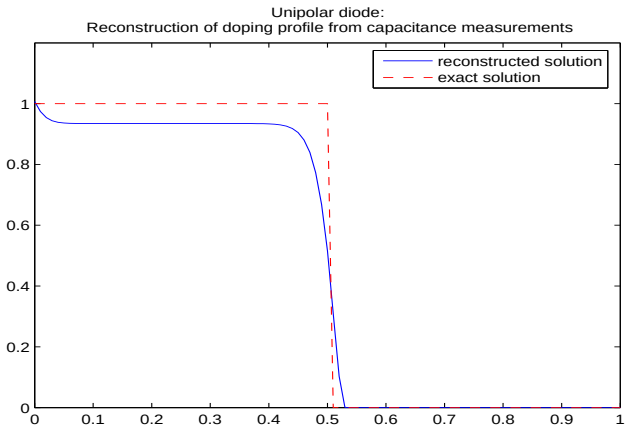

Figure 7.9: Reconstructed doping profile from capacitance measurements

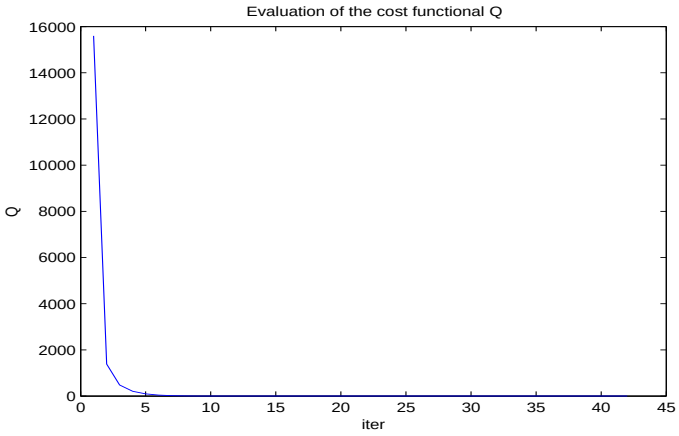

Figure 7.10: Evolution of cost functional Q

We point out that the solution is not as good as the one obtained by current measurements, the value of the cost functional Q after 40 iterations is approxi-

mately 10^{-4}. The evaluation is more time consuming as in the case of current measurements, because one has to numerically integrate (4.53).

7.2 n^+nn^+ Diode

A n^+nn^+ Diode is the combination of a higher doped n-region, a lower doped n-region and another higher doped n-region. This device can be described using the drift - diffusion equations for a unipolar device given by (7.1). The corresponding doping profile is given by:

$$C(x) = \begin{cases} 1 & 0 \leq x \leq 0.3 \\ 0.1 & 0.3 < x < 0.7 \\ 1 & 0.7 < x \leq 1 \end{cases}$$

The value of the applied potential was the same as in the case of a unipolar diode. After three iterations the reconstruction stopped because the calculated gradient was no descent direction. Figure 7.11 shows the reconstructed doping profile after 3 iterations, Figure 7.12 the gradient evaluation for this doping profile.
Solving at the adjoint equations

$$-\lambda_1 - \frac{\partial \lambda_2}{\partial t} - \mu_n \frac{\partial^2 \lambda_2}{\partial x^2} - \mu_n \frac{\partial V}{\partial x}\frac{\partial \lambda_2}{\partial x} = 0$$
$$\lambda^2 \frac{\partial^2 \lambda_1}{\partial x^2} + \mu_n n \frac{\partial^2 \lambda_2}{\partial x^2} = 0$$

one obtains that λ_2 is almost linear and that λ_1 is proportional to the gradient of the electric potential. The gradient is amplified by the value of μ_n and therefore dominates the whole equation system.
In the case of capacitance measurements no numerical problems occurred. The parameters are the same as before. As already mentioned the reconstruction from capacitance measurements is more time consuming as in case of current measurements due to the evaluation of (4.53). The reconstructed doping profile and the evolution of the cost functional can be seen in Figure 7.13 and Figure 7.14.

We started with a good initial guess (green chain dotted line in Figure 7.11 or

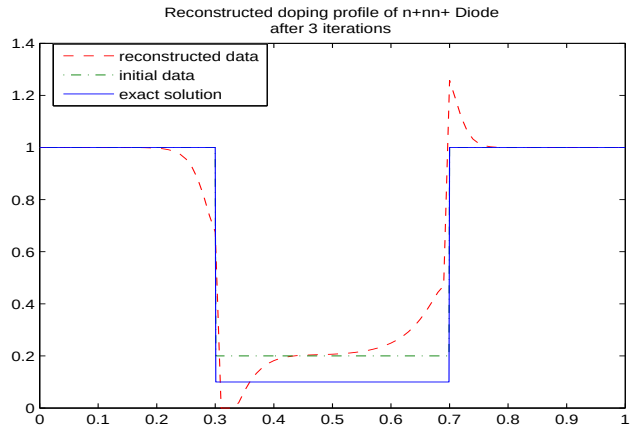

Figure 7.11: Reconstructed doping profile of a n^+nn^+ Diode after 3 iterations

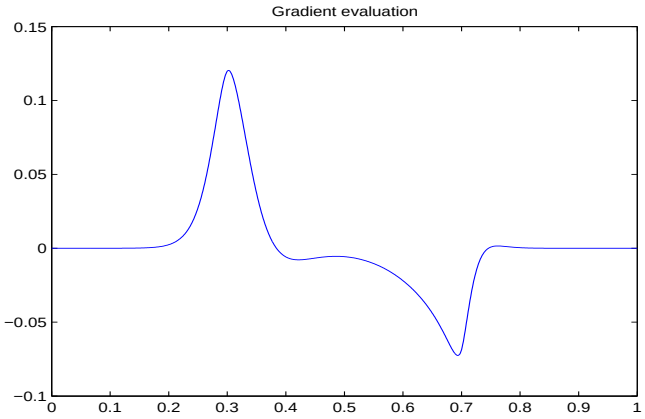

Figure 7.12: Gradient Evaluation after 3 iterations

7.13). In order to obtain reasonable results one has to know the exact values of the discontinuities.

Using capacitance measurements we needed circa 80 iterations to achieve a solution, which took about 9 hours !

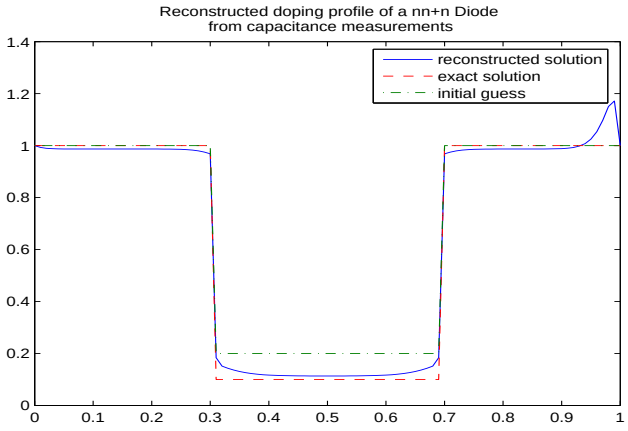

Figure 7.13: Reconstructed doping profile of a n^+nn^+ Diode

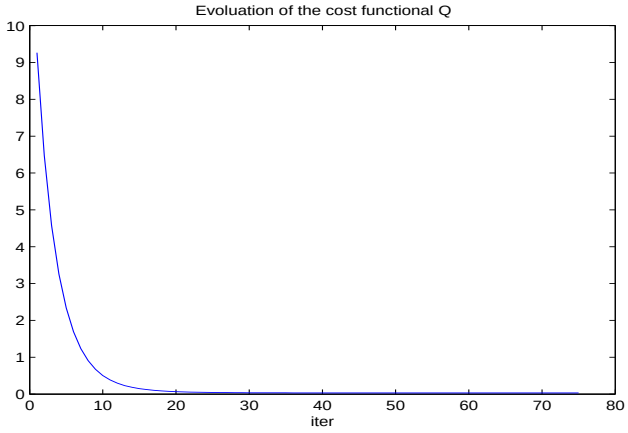

Figure 7.14: Evolution of the cost functional Q

7.3 np-Diode

We consider a semiconductor device of length $L = 10^{-4}$ cm and a maximum doping concentration $\tilde{C} = 10^{16}$ cm^{-3} . By setting $\tau_n = \tau_p = 1e^{-6}$ and $\mu_n = \mu_p = 1000$ one allows the existence of multiple solutions described in Section 5.
The exact doping profile is given by

$$C(x) = \begin{cases} 1 & 0 \leq x \leq 0.5 \\ -0.5 & 0.5 < x \leq 1 \end{cases}$$

the initial guess by

$$C_0(x) = \begin{cases} 1 & 0 \leq x \leq 0.5 \\ -0.3 & 0.5 < x \leq 1 \end{cases}$$

In Figure 7.15 the two possible solutions that produce the same total current are illustrated. In Figure 7.16 the gradient of the initial guess is shown - this gradient would be a steepest descent direction for the second solution not for the first.
In the second example we set $\mu_n = 1500$ and $\mu_p = 1000$. Furthermore when considering the symmetric doping profile

$$C(x) = \begin{cases} 1 & 0 \leq x \leq 0.5 \\ -1 & 0.5 < x \leq 1 \end{cases}$$

the two possible solutions are identical. In this case we could reconstruct the doping profile using Tikhonov regularization. The reconstructed solution is displayed in Figure 7.17, the corresponding cost functional Figure 7.18. After 90 iterations a solution was achieved - this took about 4 hours. The results are quite good, due to regularization the reconstructed solution is smoother than the exact one, the value of the cost functional is about 10^{-5}.

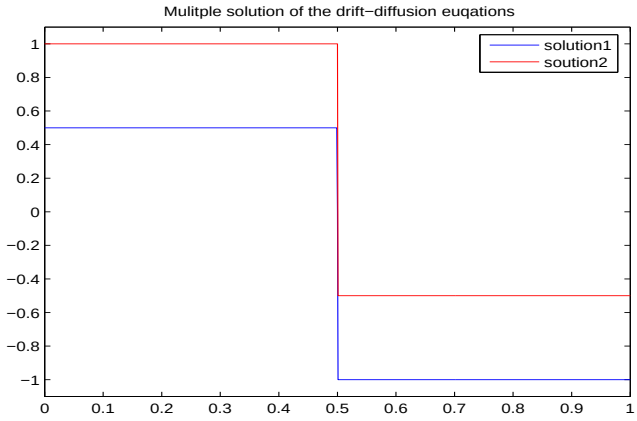

Figure 7.15: Multiple solutions of the drift - diffusion equations

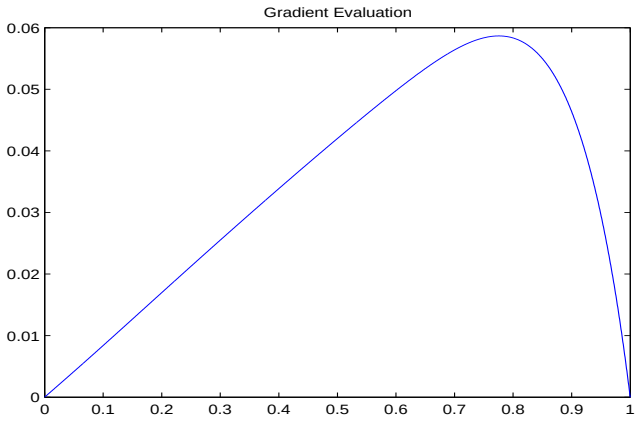

Figure 7.16: Gradient Evaluation

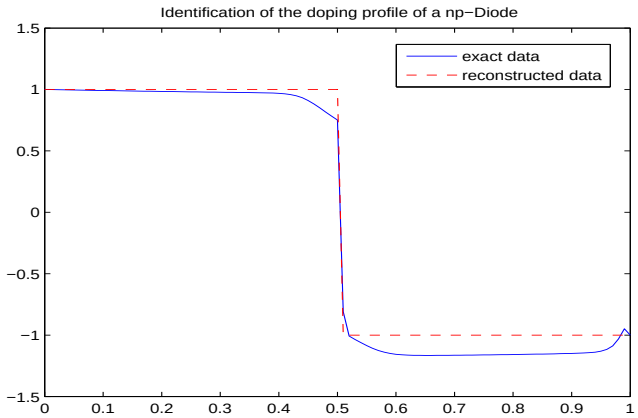

Figure 7.17: Reconstruction of the doping profile of a n-p Diode using steepest descent

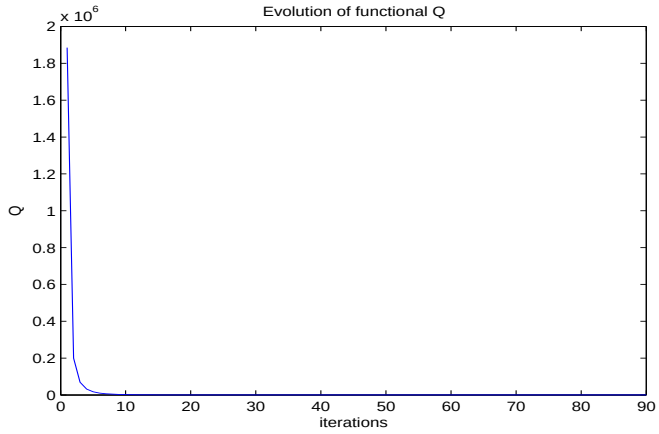

Figure 7.18: Evolution of the cost functional Q

Chapter 8

Conclusions and further work

In this work an approach to the reconstruction of semiconductor dopant profile form transient measurements is presented. The underlying analysis is discussed and numerical examples are performed using FEMLAB and MATLAB.
Considering unipolar diodes good numerical performance can be observed, especially for the case of n-diodes. For n^+nn^+ diodes the reconstruction of the dopant profile from current measurements failed, but reasonable results can be obtained using capacitance measurements.
Due to multiple solutions of the inverse doping problem numerical difficulties occurred during gradient evaluation in case of np-diodes. There has been no work on the identifiability of the dopant profile for pn-diode from transient measurements yet, which is a point of further investigation.
Therefore points of further interest are:

1. Extension to the two dimensional model for unipolar diodes
2. Solver of the asymptotic model of the drift-diffusion equations for bipolar devices
3. Investigation of the identifiability of the dopant profile from transient measurements in the case of pn-diodes

Bibliography

[1] Acar R. and Vogel C.R., Analysis of bounded variation penalty methods for ill-posed problems, *Inverse Problems* **10** (1994), 1217-1229

[2] Burger M., Engl H.W., Leitao A. and Markowich P.A. , On inverse problems for semiconductor devices, *Milan Journal of Mathematics* **72** (2004), 274-313

[3] Burger M., Engl H.W., Markowich P.A. and Paola Pietra, Identification of doping profiles in semiconductor devices, *Inverse Problems* **17** (2001), 1765-1795

[4] Burger M., Engl H.W. and Markowich P.A. , Inverse doping problems for semiconductor devices, *Recent progress in computational and applied PDEs* Kluwer Academic Publishers (2002), 27-38

[5] Burger M. and Pinnau R., Fast optimal design of semiconductor devices, *SIAM J. Appl. Math.* **64** (2003), 108-126

[6] John R. Cannon, *The One-Dimensional Heat Equation*, Addison-Wesley Publishing Company , Menlo Park (1984)

[7] Dobson D. and Scherzer O., Analysis of the regularized total variation penalty methods for denoising, *Inverse Problems*, **12** (1996), 601-617

[8] Engl H.W., Hanke M. and Neubauer A., *Regularization of Inverse Problems*, Kluwer Vienna (1996)

[9] Fang W. and Ito K., Reconstruction of semiconductor doping profile from laser-beam-induced current image, *SIAM J. Appl. Math.* **54** (1994), 1067-1082

[10] Fletcher R. , *Practical Methods of Optimization. Vol II: Constrained Optimization*, John Wiley, Chichester-New York-Brisbane-Toronto (1981)

[11] Gajewski H., On existence, uniqueness and asymptotic behavior of solutions of the basic equations for carrier transport in semiconductors, *Z. angew. Math. Mech.* **65** (1985), 101-108

[12] Giles M.B. and Pierce N.A., An introduction to the adjoint approach to design, *Flow. Turbulence and Combustion* **65** (2000), 393-415

[13] Gill P.E. , Murray W. and Wright H.M., *Practical Optimization*, Academic Press, New York (1981)

[14] Hinze M. and Pinnau R., Multiple solutions to a semiconductor design problem, SFB609-Preprint-01-2005, TU Dresden 2005 (Submitted)

[15] Hinze M. and Pinnau R., An optimal control approach to semiconductor design, *Math. Mod. Meth. Appl. Sc.* **12** (2002), 89-107

[16] Markowich P.A., *The Stationary Semiconductor Device Equations*, Springer Vienna (1986)

[17] Markowich P.A., Ringhofer Ch.A. and Schmeisser Ch., *Semiconductor Equations*, Springer Vienna (1990)

[18] Markowich P.A. and Ringhofer Ch.A., Stability of the linearized transient semiconductor device equations, *Z. angew. Math. Mech.* **67** (1987), 319-332

[19] Ringhofer Ch., An asymptotic analysis of a transient pn-junction model, *Siam J. Applied Math.* **47** (1987), 624-642

[20] Rudin L., Osher S. and Fatemi E., Nonlinear total variation based noise removal algorithms, *Physica D: Nonlinear Phenomena*, Vol. 60, Issues 1-4 (1992)

Appendix A

Notation

Sets

Name	Signification
$\mathbb{R}$	set of real numbers
Ω	domain in $\mathbb{R}^d,\ d = 1, 2, 3$
$\Gamma = \partial\Omega$	boundary of domain Ω
$T = [0, t]$	time interval

Calculus Symbols

Name	Signification
$\frac{du}{dt}$	Total derivative of a function u with respect to t
$\frac{\partial u}{\partial t}$	Partial derivative of a function u with respect to t
$\nabla u,\ \operatorname{grad} u$	Gradient of a function u
Δu	Laplacian of a function u
$\int_\Omega u\, dx$	Volume integral of a function u over Ω
$\int_{\partial\Omega} u\, ds$	Surface integral of a function u over $\partial\Omega$

Function Spaces

$C(\Omega)$	Space of continuous functions
$C^k(\Omega)$	Space of continuous functions with continuous derivatives up to the order k
$C^{k,\alpha}(\Omega)$	Space of continuous functions with Hölder continuous derivatives up to the order k with Hölder exponent α
$C_b^k(\Omega\ )$	Space of continuous and bounded functions with continuous and bounded derivatives up to the order k

Space of p-times integrable real-valued functions:
$L^p(\Omega) = \left\{u(x) - \text{measurable} \mid \|u\|_{L^p(\Omega)} = \left(\int_\Omega |u|^p\, dx\right)^{\frac{1}{p}} < \infty\right\}$
$L^\infty(\Omega) = \{u(x) - \text{measurable} \mid \text{ess sup}\, |u(x)| < \infty\}$

Sobolev space of real-valued functions with p-integrable derivative up to the order k:
$W_p^k(\Omega) = \{u \in L^p(\Omega) \mid \partial^\alpha u \in L^p(\Omega), \forall \alpha : 0 \leq |\alpha| \leq k\}$

$H^k(\Omega)$	Sobolev space $W_2^k(\Omega)$

List of Figures

List of Tables